Nuclear Engineering and Design 358 (2020) 110386

Contents lists available at ScienceDirect

Nuclear Engineering and Design

journal homepage: www.elsevier.com/locate/nucengdes

TALL-3D open and blind benchmark on natural circulation instability

D. Grishchenko[a,*], A. Papukchiev[b], C. Liu[d], C. Geffray[c], M. Polidori[e], K. Kööp[a], M. Jeltsov[a], P. Kudinov[a]

[a] Division of Nuclear Engineering, Royal Institute of Technology, Roslagstullsbacken 21, SE-106 91 Stockholm, Sweden
[b] Gesellschaft fuer Anlagen- und Reaktorsicherheit (GRS) gGmbH, Boltzmannstr. 14, D-85748 Garching, Germany
[c] French Alternative Energies and Atomic Energy Commission (CEA), DEN/DM2S/STMF – Service de Thermohydraulique et de Mécanique des Fluides, Université Paris-Saclay, F-91191 Gif-sur-Yvette, France
[d] Department of Nuclear Engineering, Faculty of Mechanical Engineering, Technical University of Munich (TUM), Boltzmannstr. 15, D-85748 Garching, Germany
[e] Italian National Agency for New Technologies, Energy and Sustainable Economic Development (ENEA), Lungotevere Thaon di Revel, 76, 00196 ROMA, Italia

ARTICLE INFO

Keywords:
TALL-3D
STH model
CFD model
Model validation
LBE experiment
Liquid metal thermal-hydraulics
Validation experiments
Model calibration

ABSTRACT

Design and safety analysis of the currently developed pool type liquid metal cooled fast nuclear reactors is currently impaired by limited operational experience for such systems and insufficient confidence in the predictive capabilities of the applied modelling. Understanding of pool-reactor thermal-hydraulics is crucial for assessment of reactor performance and passive safety systems reliability. Credibility of the analysis tools can be established in the process of code validation, which includes open and blind benchmarks against integral experiments.

TALL-3D is a lead-bismuth eutectic (LBE) loop built to provide experimental data for validation of standalone and coupled system thermal-hydraulics (STH) and computational fluid dynamics (CFD) codes. This paper summarizes the results of the open and blind benchmark exercise, performed using experimental data on natural circulation instability in liquid metal flows from the TALL-3D facility.

An approach for selection of experimental data for benchmark and tests for model input calibration is presented. A list of parameters, initial and boundary conditions are defined based on modelling limitations and sources of experimental uncertainty. A set of requirements and assessment criteria for the blind calculations were specified. Results of simulations are compared to experimental data. Implications of the benchmark test results for the codes validity and lessons learned are reported.

1. Introduction

High safety requirements setup at Gen-IV International Forum (Gen-IV, 2008) for the advanced nuclear energy generation systems impose strict requirements to the validity (predictive capability) of the numerical tools used for the design and safety analyses of the future reactors. Furthermore, pool-type design, motivated by passive safety, non-proliferation and ease of deployment, challenges applicability of "conventional" standalone STH codes and requires CFD analysis. High computational efforts associated with CFD currently prevent CFD application to the complete flow domain. As a trade-off between computational efficiency and physical accuracy coupled STH/CFD approaches are being developed (Jeltsov et al., 2013; Cadinu and Kudinov, 2009; Papukchiev and Lerchl, 2009) and applied. Coupling, however, introduces additional level of modelling that can be a source of important uncertainty or error. Additionally, modelling of the thermal-hydraulics of future reactors is challenged by (i) multiscale phenomena (appropriate user selection of models and approaches for turbulence simulation (DNS/LES/RANS) in CFD) and (ii) usage of novel materials that require specification of non-dimensional parameters. This further enhances concerns about the validity and accuracy of used numerical tools, especially with respect to the safety analysis.

Considering the ongoing change in the paradigm of safety assessment from conservative to the best estimate plus uncertainty, validation and quantification of model uncertainty became one of the most vital issues in the last decade. Adequate demonstration of code/model performance is commonly achieved by comparison of model predictions against relevant experimental data in open and blind benchmarks. In this paper, we summarize the results of the first round of open and blind benchmark exercises performed within the framework of Horizon 2020

* Corresponding author.
E-mail addresses: dmitrygr@kth.se (D. Grishchenko), angel.papukchiev@grs.de (A. Papukchiev), chunyu.liu@tum.de (C. Liu), clotaire.geffray@cea.fr (C. Geffray), massimiliano.polidori@enea.it (M. Polidori), koop@kth.se (K. Kööp), jeltsov@kth.se (M. Jeltsov), pkudinov@kth.se (P. Kudinov).

https://doi.org/10.1016/j.nucengdes.2019.110386
Received 27 June 2019; Received in revised form 18 September 2019; Accepted 11 October 2019
Available online 15 November 2019

Acronyms

CFD	Computation Fluid Dynamics
DAS	Data Acquisition System
FM	Flowmeter
FR	Flow Rate
HTC	Heat Transfer Coefficient
HX	Heat eXchanger
LBE	Lead-Bismuth Eutectic
LCO	Limit Cycle Oscillations
LES	Large Eddie Simulations
MH	Main Heater
PFL	Pressure Flow Loss coefficient
RANS	Reynolds-Averaged Navier–Stokes (equations)
SRQ	System Response Quantity
STH	System Thermal Hydraulic
TC	Thermocouple
TG	Test Group
UQ	Uncertainty Quantification

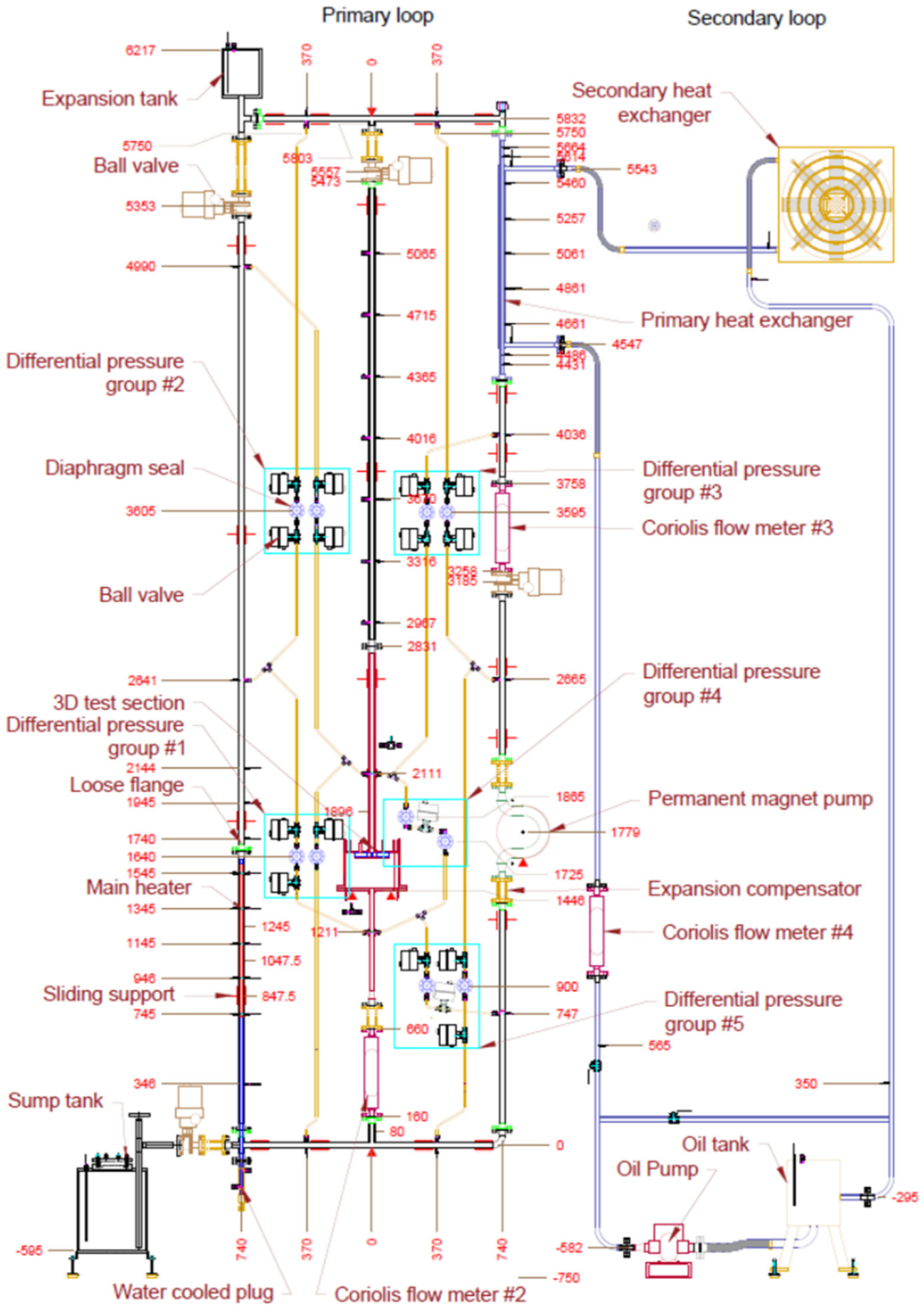

Fig. 1. TALL-3D facility main components.

EC SESAME (Thermal-Hydraulics Simulations and Experiments for the Safety Assessment of MEtal Cooled Reactors) Project as one of the steps towards understanding of the current modelling capabilities with respect to thermal-hydraulics of heavy metals.

Specifically, standalone and coupled models developed by different SESAME project partners were tested against transient and steady state experimental data from the TALL-3D facility. The goal of this work is to (i) evaluate the maturity level of modelling (from perspective of both predictive capability of numerical tools employed and approaches to establishing such capability) and (ii) provide a guidance for future benchmark and validation exercises.

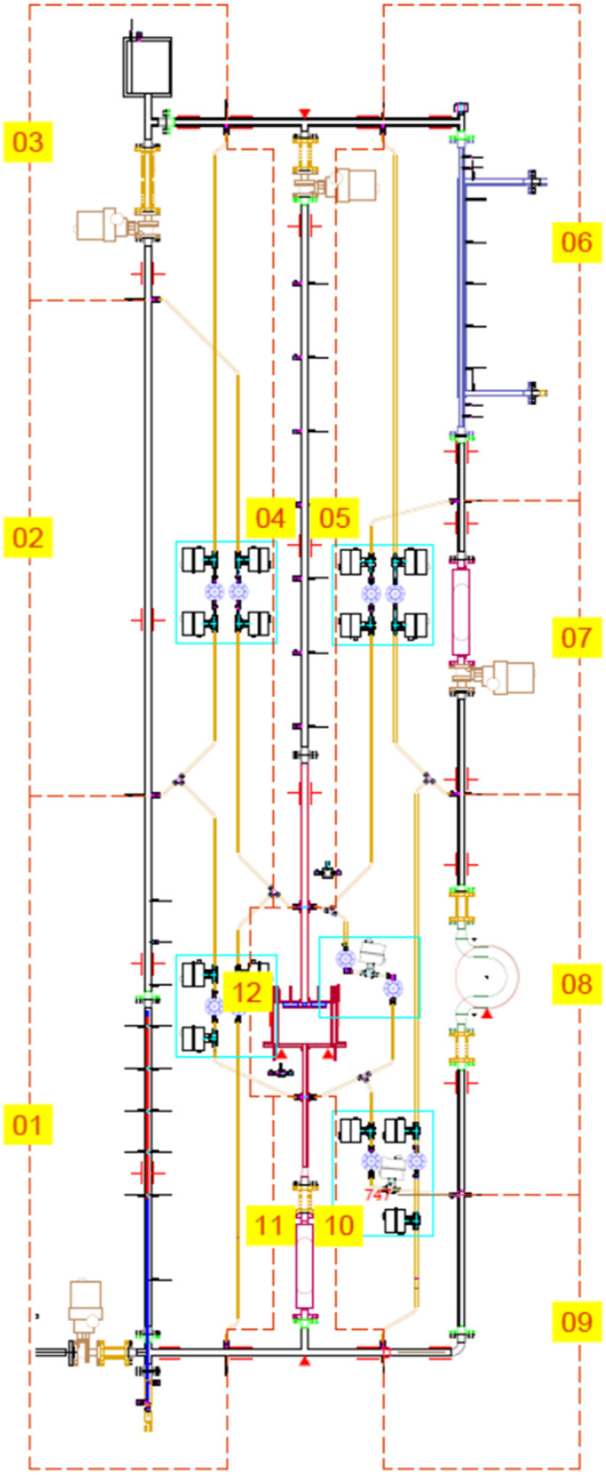

a

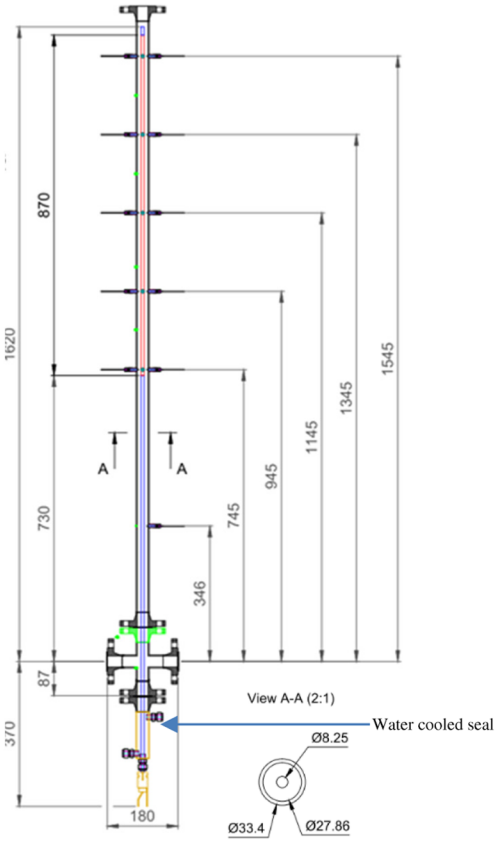

b

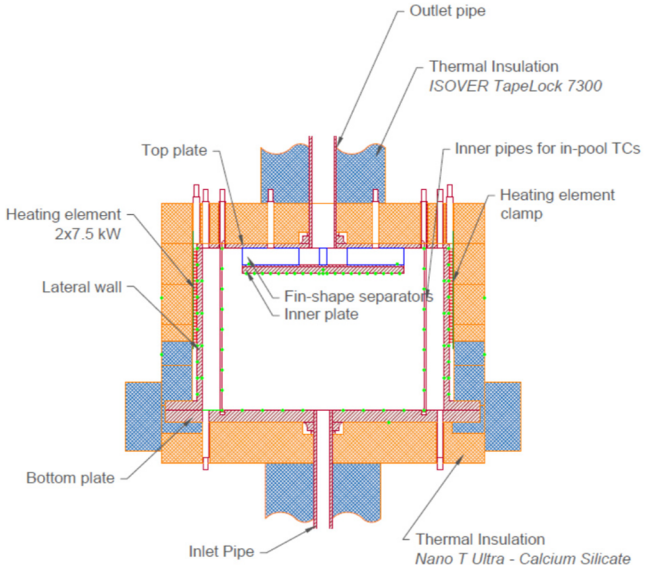

c

Fig. 2. TALL-3D facility sectioning (a), main heater (b) and the test section (c).

Table 1
Main loop sections and instrumentation.

Section	Leg	Components	DP group	Section Inlet/Outlet TCs: TC [leg].[Elevation]	Flow meter
1	MH	Lower left elbow and main heater	DP1	TC1.0000/TC2.2641	FHX-F3D*
2	MH	Vertical pipe on MH leg	DP2	TC1.4990/TC2.2641	FHX-F3D
3	MH	Upper left elbow, ball valve, expansion compensator, expansion tank	DP2	TC1.4990/TC1.5830	FHX-F3D
4	MH, 3D	Upper left T-junction, ball valve	DP2	TC1.5830/TC2.2111	FHX-F3D, F3D
5	HX, 3D	Upper right T-junction, ball valve	DP3	TC3.5830/TC1.2111	FHX,F3D
6	HX	Upper right elbow, Heat exchanger	DP3	TC3.5830/TC3.4036	FHX
7	HX	Flow meter #3, and ball valve	DP3	TC3.2665/TC3.4036	FHX
8	HX	EPM pump and 2 expansion compensators	DP5	TC3.2665/TC3.0747	FHX
9	HX	Lower right elbow	DP5	TC3.0000/TC3.0747	FHX
10	HX, 3D	Lower right T-junction, flow meter #2	DP5	TC3.0000/TC2.1211	FHX, F3D
11	MH, 3D	Lower left T-junction, flow meter #2	DP1	TC1.0000/TC2.1211	FHX-F3D, F3D
12	3D	3D test section	DP4	TC2.1211/TC2.2111	F3D

* F3D – flow meter on 3D leg (FM2); FHX – flow meter on the HX leg (FM3).

Table 2
Ranges of dimensionless numbers.

Dimensionless number	Minimum value	Maximum value
	Main loop	
$Re = \rho \bullet v \bullet D/\mu$	0	140 000 220 000 (TS inlet pipe)
$Pr = C_p \bullet \mu/k$	0.020	0.054
$Pe = Re \bullet Pr$	0	342
	Test section pool	
Re	0	12 500
$Ri = Gr/Re$	0 (no heater)	1000 (natural circulation)
$Gr = \rho \bullet g \bullet \beta \bullet \Delta T \bullet D^3/\mu$	0 (no heater)	1E12

2. Experimental setup

The experimental facility was designed for the purpose of coupled and standalone code calibration, benchmarking and validation. The key requirements to the experimental setup were formulated as follows:

- Mutual feedback between 1D (STH) and 3D (CFD) components to allow validation of coupling algorithms/coupled codes.
- Separation of the facility on adjacent sections with complete boundary conditions measured for every section:
  - o section-wise calibration, benchmarking and validation of standalone codes.
- Multiple measurement points to provide:
  - o sufficient number of constrains for model calibration
  - o sufficient number of system response quantities (SRQs) for model validation
- Multiple operation regimes:
  - o sensitivity of experimental SRQs to initial and boundary conditions:
  - o separation of calibration and validation data.
- Sufficient accuracy of experimental measurements for quantitative validation.
- Phenomenological scalability:
  - o results of model validation must be applicable for code validation.

Table 4
List of benchmark participants and provided results.

Member	UQ	Benchmark			
		Blind phase	Open phase		
		S301.03	S301.03	S10.01	S301.04
CEA	no	CATHARE/ TRUST	–	CATHARE	CATHARE/ TRUST
GRS	no	ATHLET/ ANSYS CFX	ATHLET/ ANSYS CFX ATHLET	ATHLET	ATHLET/ ANSYS CFX ATHLET
TUM	yes	ATHLET/ ANSYS CFX ATHLET	ATHLET/ ANSYS CFX ATHLET	ATHLET	ATHLET/ ANSYS CFX ATHLET
ENEA	no	CATHARE	CATHARE/ TrioCFD	CATHARE	CATHARE

Table 3
List of TG03 tests and tests conditions.

#	Name	Initial steady state → final steady state				Oil temperature	Oil flow rate
		HX mass flow rate	TC3.5830	MH power	TS power		
		kg/sec	°C	kW	kW	°C	kg/s
1	TG03.S301.01	4.6 → 0.5	245 → 270	3.2 → 3.2	5.5 → 5.5	61.5	1
2	TG03.S301.02	4.6 → 0.5	227 → 245	2.5 → 2.5	4.9 → 4.9	62.5	1
3	**TG03.S301.03**	**4.7 → xxx**	**288 → xxx**	**0.72 → 0.72**	**10.3 → 10.3**	**126**	**1**
4	**TG03.S301.04**	**3.3 → 0.5**	**250 → 280**	**3.2 → 3.2**	**4.0 → 4.0**	**86**	**0.25**
5	TG03.S301.05	3.3 → 0.53	250 → 284	3.2 → 3.2	4.2 → 4.2	86	0.26
6	TG03.S301.06	4.8 → 0.59	292 → 335	1.1 → 1.1	10.6 → 10.6	116	0.98
7	TG03.S301.07	4.8 → 0.4	241 → 255	0.45 → 0.45	5.6 → 5.6	133	0.92
8	TG03.S302.01	4.3 → 0.5	182 → 271	2.3 → 2.3	0 → 4.9	141	0.95
9	TG03.S306.01	0.5 → 4.6	244 → N/A	2.5 → 2.5	4.8 → 4.8	62.5	1
10	TG03.S307.01	0.5 → 4.6	269 → 240	3.2 → 8.6	5.5 → 0	62	1
11	**TG03.S310.01**	**4.6 → 0.5**	**241 → 274**	**8.6 → 8.6**	**0 → 0**	**62**	**1**
12	TG03.S311.01	0.5 → 0.45	280 → 290	3.2 → 0.6	4.0 → 6.7	86	0.25

Items in bold correspond to the tests selected for the benchamrk.

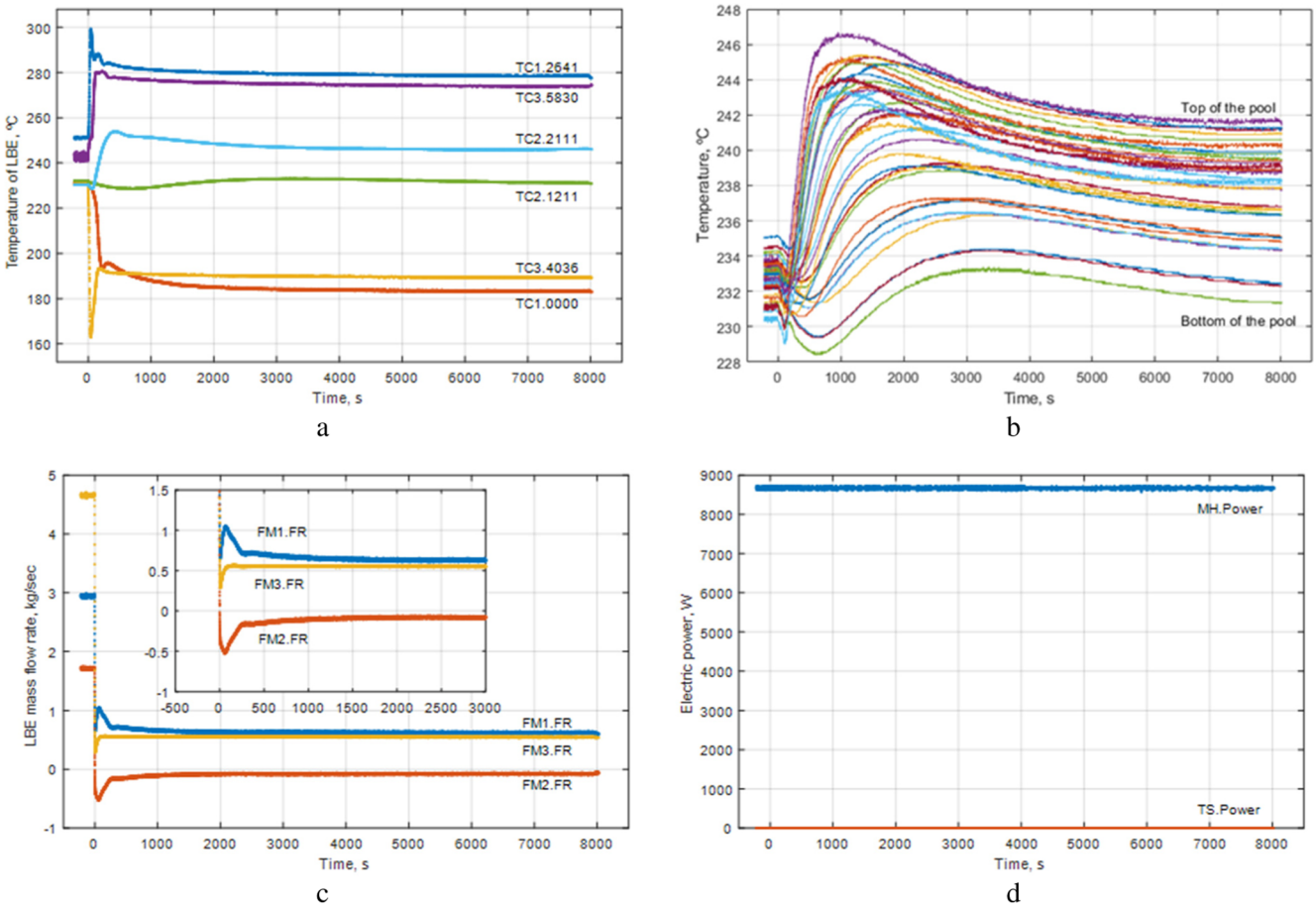

Fig. 3. Open STH benchmark test TG03.S310.01. (a – LBE loop temperatures; b – vertical in-pool temperatures; c – mass flow rates; d – electric powers).

The schematic of the TALL-3D installation is shown in Fig. 1. It incorporates the primary loop, the secondary loop, the differential pressure measurement system and pressurized service loop (not shown). The working fluid in the primary loop is LBE. LBE is characterized by low melting point (125 °C) which is suitable for experiments with temperature-sensitive instrumentation. All facility components that come in contact with LBE are made of 316L stainless steel and are equipped with band, tape or rope type heaters.

The primary loop consists of the sump tank (Fig. 1) used to store, melt and supply LBE into the loop and 3 connected vertical legs: Main Heater leg (left), 3D leg (middle), and Heat Exchanger leg (right).

The Main Heater (MH) leg accommodates (i) the pin-type 27 kW electric heater (outer diameter 8.2 mm, heated length 870 mm) in the lower part, and (ii) the expansion tank at the top. The expansion tank is used to (i) maintain loop pressure during temperature induced volumetric change of the loop components and LBE and (ii) to monitor the LBE level in the loop.

The 3D leg connects a pool-type test section to the loop. The test section is a cylindrical stainless steel vessel (Fig. 2c). At the top, the test section is equipped with an external 15 kW rope heater. A disk shaped plate is positioned inside the pool to enhance flow mixing. More than 150 thermocouples (TCs) are installed in the test section to measure wall and flow temperatures at different locations (green points in the Fig. 2c). These measurements are for validation of CFD models.

The design of the test section is intended to satisfy the key requirement for validation of coupled codes, i.e. provide mutual feedback between the TS (modelled with CFD) and the rest of the loop (modelled with STH). Depending on LBE mass flow rate and power of the test section heater, the pool inside the test section can undergo thermal mixing or stratification – phenomena that in transient can only be captured by a CFD code or STH with 2D/3D modules like ATHLET (Schoeffel et al., 2014) and CATHARE (Robert et al., 2003). Transient pool characteristics determine LBE temperature at the test section outlet (and inlet in case of flow reversal) and affect buoyancy driven flow in the entire loop. In coupled codes the test section constitutes the CFD domain of the facility, while the rest of the loop belongs to the STH domain. The boundaries between the domains are defined at the inlet (elevation 1211 mm) and outlet (elevation 2111 mm) of the test section (see Fig. 1). The data that is continuously recorded at these boundaries includes LBE flow temperature, differential pressure over the section and LBE mass flow rate.

The Heat Exchanger (HX) leg (right) has (i) the counter-current double-pipe heat exchanger (Fig. 2b) placed at the top and (ii) the Electric Permanent Magnet (EPM) pump at the bottom. The heat removal capacity of the heat exchanger exceeds 15 kW. Common flow direction in the primary loop is downwards in HX leg, and upwards in the MH and the 3D legs. Vertical legs are equipped with ball valves that provide a possibility to isolate individual legs as well as to control hydraulic resistances. Thermal expansion of the facility is allowed in horizontal direction, but restricted in vertical direction by means of

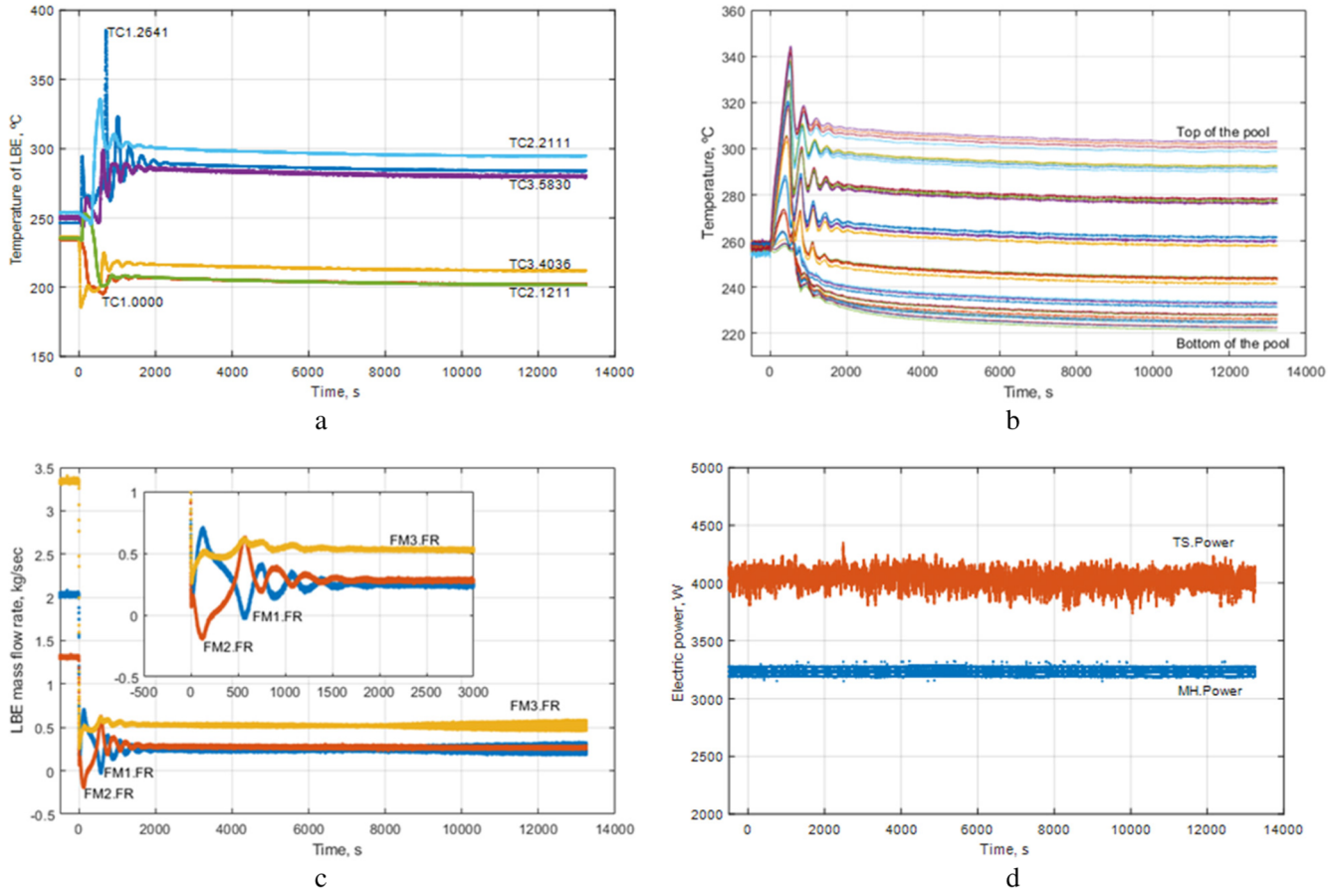

Fig. 4. Open benchmark test for coupled STH/CFD codes TG03.S301.04. (a – LBE loop temperatures; b – vertical in-pool temperatures; c – mass flow rates; d – electric powers).

expansion compensators. This is required to minimize the effect of hydrostatic head variation during transients due to thermal expansion of the loop. During loop operation temperatures up to 500 °C, pressures up to 0.7 MPa and flow rates up to 5 kg/s (flow velocity of ~2.6 m/s at the 3D section inlet) can be established.

Following the above requirements to an experimental setup for code validation, we started with separating the facility into 12 adjacent sections (Fig. 2a). For each section, inlet and outlet flow temperature, differential pressure drop and mass flow rate measurements were provided (see Table 1). This allows separate study of individual sections and section-wise calibration of model input parameters. Most of the sections are equipped with additional measurement of the local LBE flow temperature thus satisfying the "multiple measurements" requirement. For example, the riser above the test section is equipped with 8 intermediate TCs to track temperature front propagation and dissipation in LBE.

The facility can be operated in forced and natural circulation and provide complex transient behavior. The complexity of the transient phenomena stems from the competing nature of the main heater and 3D legs in buoyancy driven flow. During natural circulation, transient recovery of the flow in the main heater leg is accompanied by flow reduction or flow reversal in the 3D leg; the same phenomena occurs in the MH during flow recovery in the 3D leg. Different LBE volumes in the main heater and in the 3D test section in combination with different heating powers provide different timings of flow recovery (thermal inertia) in these legs resulting in development of multiple flow oscillations during transients. Depending on the ratio of the powers in the main heater and test section heater, the amplitude of flow oscillations between the competing legs can be decreasing, increasing, or continuous (limit cycle oscillations), thus allowing to operate the facility in different regimes.

Main thermal–hydraulic characteristics of the loop are provided in Table 2 as a set of dimensionless numbers. The intervals are provided assuming 0 to 5 kg/s mass flow rate and 150 to 350 °C LBE flow temperature.

More details on the TALL-3D experimental setup can be found in (Grishchenko et al., 2014).

3. Benchmark program

The complete set of transient tests performed on TALL-3D facility for benchmarking is provided in the Table 3. This set does not include the test groups TG00-02, which were specifically dedicated to commissioning, quantification of measurement uncertainty and calibration (Grishchenko et al., 2017). Among the 12 transient tests listed in the Table 4 three were selected for benchmarking:

- TG03.S301.03 – semi-blind benchmark test for coupled STH/CFD or standalone STH code
- TG03.S301.04 – open benchmark test for coupled STH/CFD
- TG03.S310.01 – open benchmark test for standalone STH

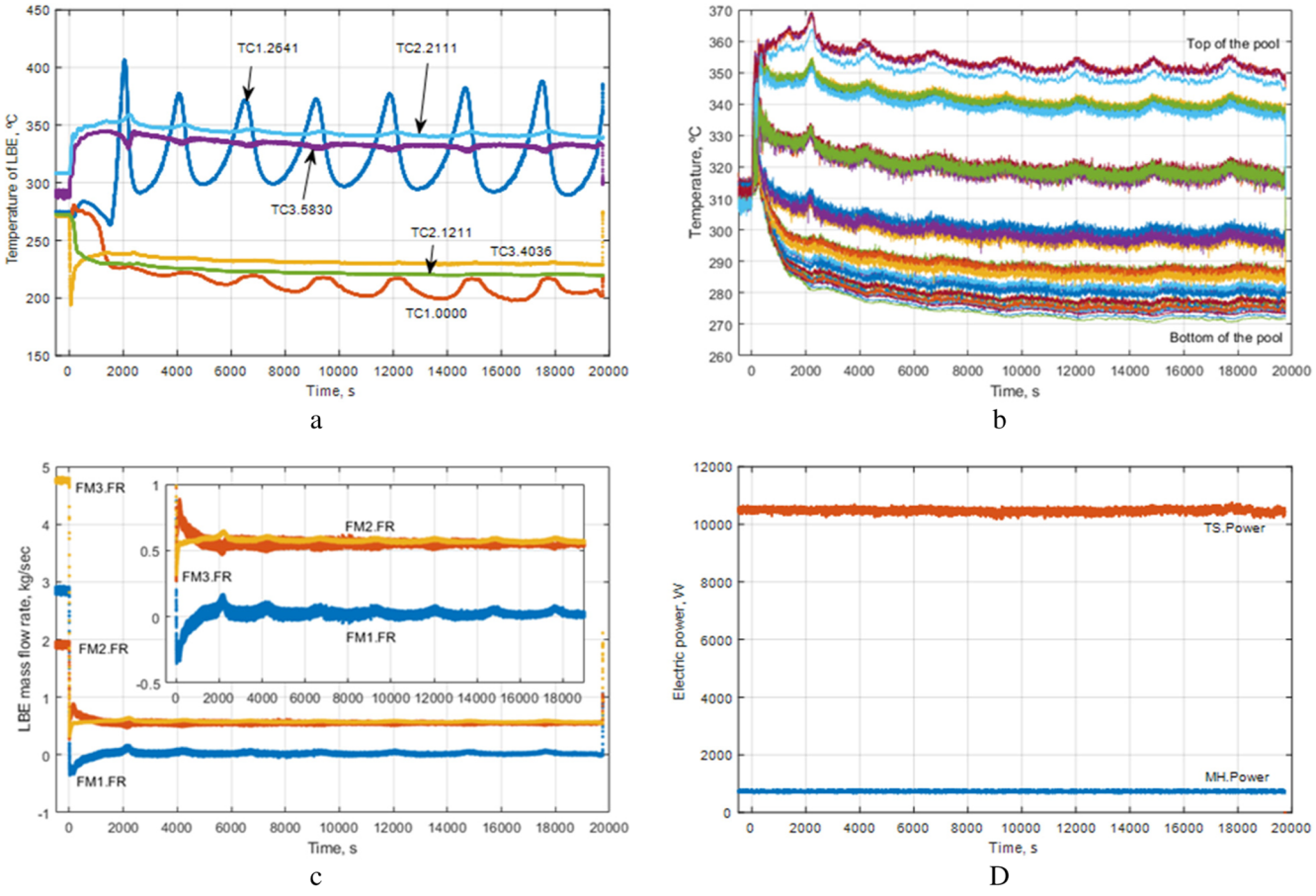

Fig. 5. Blind benchmark test TG03.S301.03. (a – LBE loop temperatures; b – vertical in-pool temperatures; c – mass flow rates; d – electric powers).

The selection was motivated by possibility to separately evaluate: (i) standalone STH modelling, (ii) coupled STH/CFD modelling and (iii) model predictive capability in semi-blind benchmark (where participants were free to choose the modelling approach). Details about selected tests are provided below.

Other tests in the series were aiming to provide to partners additional (to calibration tests) insights into transient responses of the TALL-3D facility to the variation in the initial conditions (heater powers, mass flow rates and temperatures) for model calibration prior to benchmarking. For example, the test TG03.S301.06 was specifically performed to provide experimental data with high (10 kW) electric power in the 3D test section – similar to the conditions in the semi-blind benchmark; test TG03.S301.07 was provided as an example of possible limit cycle oscillations that can develop between the Main Heater and 3D leg given specific electric power distribution between the MH and the 3D test section.

In this work we left out the details of model calibration done by the participants. For the validation metric we compare mass flow rates in individual legs and inlet/outlet temperatures around main components in these legs: main heater, test section and heat exchanger. Definition of unified quantitative SRQs for comparison of partners results turned out to be partially unnecessary.

3.1. Benchmark tests

3.1.1. Open STH benchmark test TG03.S310.01

TG03.S310.01 is a forced to natural circulation transient with zero electric power in the 3D test section and almost 9 kW power in the MH (Fig. 3). Since no heating of the 3D pool is applied, there is no external driver for the pool thermal stratification, making this transient best-suited for standalone STH modelling and validation. Main aspects of the transient are:

- Fast transition to the steady state (8000 s)
- No flow oscillations between the MH and 3D leg.
- Continuous flow reversal in the 3D leg
- Test section acting as a flow cooler
- Minor change during the transient in the pool vertical temperature gradient: 0.01 → 0.05 K/mm (compared to stratified case 0.01 → 0.2 K/mm)

STH modelling of this test is essentially resolving two steady states; deficiencies in the modelling of the transient might be difficult to identify due to very short transition period, which can be affected by the run-down time and the thermal effect of the pump.

Table 5
List of codes and models setup used by different partners.

Code	Name	Version	Dim	Turbulence model	Turbulent Prandtl number	Cell size	Number of elements	Time step	UQ method	Sample size
CEA										
CFD	TRUST	1.7.6	2D	k-e	0.9	avg 0.3 cm	422,457	adaptive (max 0.5, min 0.001)	–	–
STH	CATHARE	v25_3 mod6.1	1D	n.a.	n.a.	10 cm	300	adaptive (max 0.5, min 0.001)	–	–
ENEA										
CFD	TrioCFD	1.7.7	2D	k-e	fixed	unstructured 2D grid with constant mesh size (about 0.8 cm)		automatic	–	–
STH	CATHARE	v25_3 mod6.1	1D	n.a.	n.a.	5–10 cm	360	automatic	–	–
CFD	TrioCFD	1.7.7	2D wedge 10°	k-e	fixed	unstructured 3D grid with constant mesh size (about 8 mm)		automatic	–	–
GRS										
CFD	ANSYS CFX	18.2	2D	SST*	0.9	0.15 cm	114,528	0.1 s	–	–
STH	ATHLET	3.0	1D	n.a.	n.a.	10 cm	260	0.05–0.5 s	–	–
TUM										
CFD	ANSYS CFX	18.0	2D	SST	0.9	0.15 cm	56,040	0.1 s	Wilks	56–120
STH	ATHLET	3.0	1D	n.a.	n.a.	10 cm	291	0.05–0.5 s		

* SST = Menter's Shear Stress Transport.

3.1.2. Open coupled code benchmark test TG03.S301.04

TG03.S301.04 is a forced to natural circulation transient with constant electric powers in the MH and 3D heaters (Fig. 4). The test was selected due to (i) pronounced flow oscillations between the MH and 3D legs, (ii) temporary flow reversal in the 3D leg, which results in a challenging for standalone STH abrupt temperature rise in the test section inlet (TC2.1211), and (iii) multiple transitions of pool between stratified and mixed conditions. Prediction of the transient requires application of coupled STH/CFD codes. The main characteristics of the transient are:

- Relatively short (3000 s) duration of flow oscillations between the MH and 3D leg
- Long time to achieve the natural circulation steady state (13000 s)
- Pool thermal stratification/mixing.

Modelling of this test is expected to properly predict (i) natural circulation steady state, (ii) frequency and decay rate of the flow oscillations following the flow reversal in the 3D leg, and (iii) transient temperature peak in the inlet to the test section during the flow reversal.

3.1.3. Semi-blind benchmark test TG03.S301.03

TG03.S301.03 is forced to natural circulation transient with constant electric power in the MH and 3D heaters (Fig. 5). The transient conditions for this test were identified in separate analytical and experimental study (Kööp et al., 2017), which was conducted to investigate the possibility of LCO (Limit Cycle Oscillations) in the TALL-3D loop. The blind benchmark test fell into the category of tests that could potentially exhibit LCO. Specifically, in the course of the test continuous flow oscillations were established in the MH leg, however, those oscillations were accompanied by temperature oscillations in the MH leg with a growing amplitude. It was not possible to run the test long enough to confirm its final state.

The test was selected due to (i) not triviality of transient response and (ii) sensitivity to the modelling of thermal losses. Main characteristics of the transient are:

- Prolonged (> 20 000 s) flow oscillations between the MH and 3D leg in natural circulation
- Increasing amplitude of temperature oscillations
- Constant conditions in the 3D pool
- Long period (1400 s) of flow recovery (reversed and stagnant flow) in the MH leg immediately after the start of the transient.
- Continuous cooling down of the primary flow.

The simulations were expected to correctly resolve (i) initial flow recovery, (ii) frequency and amplitude of flow oscillations, and importantly, (iii) the temperature evolution in the MH and 3D legs.

In the TG03.S301.03 test, right after transition to the natural circulation, the LBE mass flow rate in the 3D leg and temperature profile in the test section pool remains largely unchanged, i.e. flow in the 3D leg (CFD domain) is close to a steady state. Without dynamic transition between mixed/stratified pool states, heat balance defines inlet/outlet temperature of the test section and a standalone STH code can be used to predict these characteristics.

3.2. Benchmark conditions and participants

The benchmark participants were asked to provide results for the three tests. The participants were encouraged to perform uncertainty quantification for all tests.

The open benchmark tests (for standalone STH and coupled STH/CFD models) were provided as recorded by the DAS (Data Acquisition System). The semi-blind benchmark included the initial steady state and initial 1100 s of the transient – the period of reversed flow in the

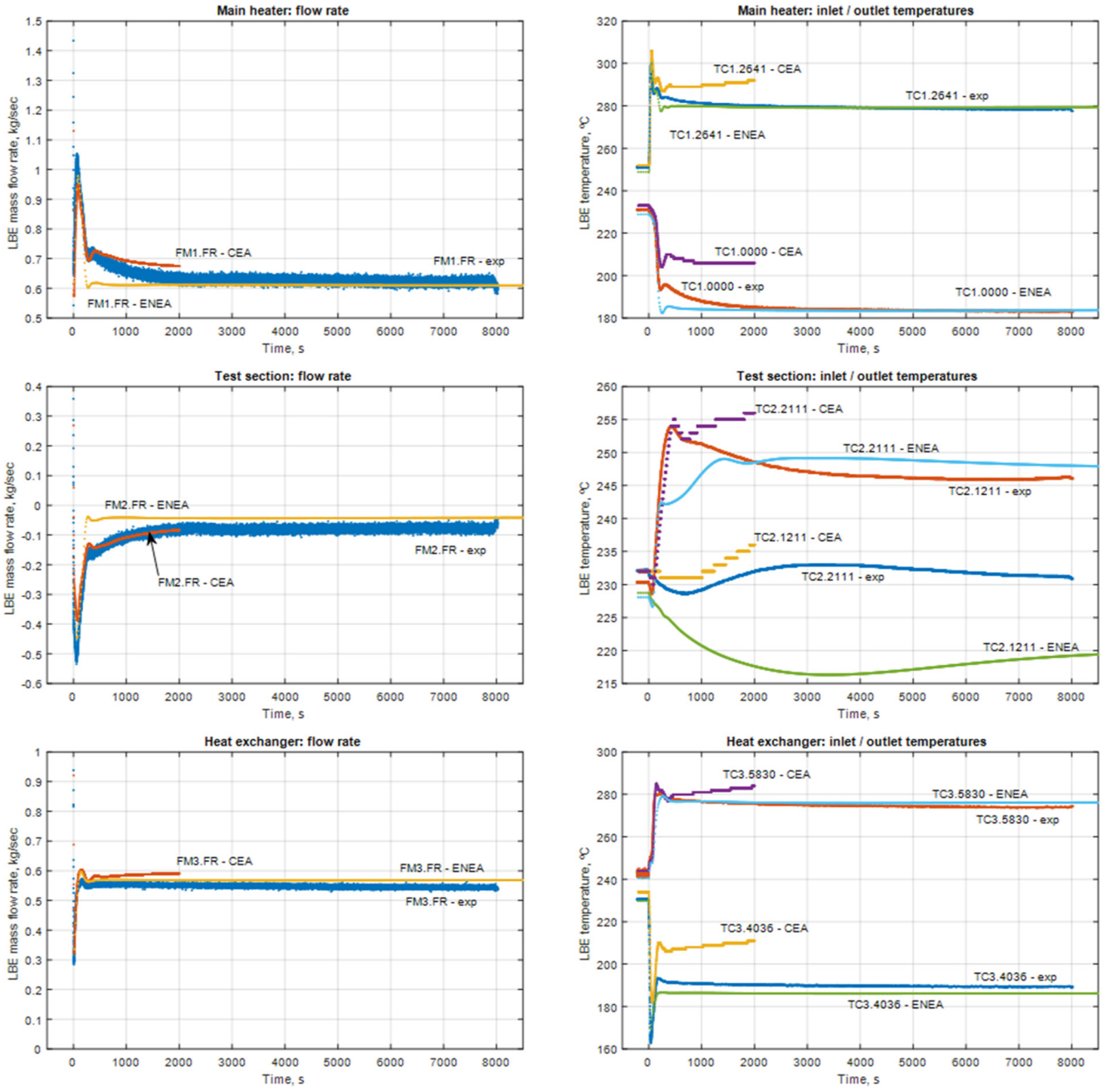

Fig. 6. ENEA and CEA simulations of the open STH benchmark (TG03.S310.01).

MH leg. In addition to that, a complete history of the secondary side of the HX was provided. The latter was necessary for calibration of thermal losses in the HX. Modelling of the semi-blind benchmark test is possible using a standalone STH or coupled STH/CFD codes, however, the decision was left to benchmark participants.

Four institutes participated in the benchmark exercise CEA, GRS, TUM and ENEA. The list of submitted simulations is provided in the Table 4. The list of used codes and some details on models setup is given in the Table 5.

4. Results and discussions

4.1. TG03.S310.01 – STH benchmark

CEA and ENEA used CATHARE code to model TG03.S310.01 transient, the results of the modelling are provided in Fig. 6. The mass flow rates in all three legs have been captured within ± 0.05 kg/s. However, prediction of the flow temperature around the test section was not successful. Possible reasons for disagreement between the experiment and simulations could be:

Table 6
TUM input uncertain parameters and ranges.

#	Parameters	Input for code	Min.	Max.	TG03.
1	Roughness of pipes in MH leg (value)	ATHLET	1.69E-05	2.63E-05	
2	Roughness of pipes in common parts (value)	ATHLET	1.69E-05	2.63E-05	
3	Roughness of pipes in HX leg (value)	ATHLET	1.69E-05	2.63E-05	
4	Roughness of pipes in TS leg (value)	ATHLET	1.91E-05	2.85E-05	
5	Roughness of pipes in Rotamass (value)	ATHLET	1.69E-05	2.63E-05	
6	Power of the MH (factor)	ATHLET	0.977	1.023	
7	Power of the TS heater (factor)	ATHLET, CFX	0.985	1.015	S301.03
8	PFL coefficient of MH leg (factor)	ATHLET	0.813	1.231	
9	PFL coefficient of EPM pump (value)	ATHLET	29.267	41.735	
10	HTC in common parts (factor)	ATHLET	0.9	1.1	
11	HTC in HX leg (factor)	ATHLET	0.9	1.1	
12	HTC in MH leg (factor)	ATHLET	0.9	1.1	
13	HTC in TS leg (factor)	ATHLET	0.9	1.1	
14	Initialization temperature at TC1.0000 (additive)	ATHLET	−2.2	2.2	
15	LBE dynamic viscosity (multiplicative)	ATHLET, CFX	0.92	1.08	
16	LBE thermal conductivity (multiplicative)	ATHLET, CFX	0.95	1.05	
17	HTC forced or natural convection to LBE (value)	ATHLET	0.85	1.15	
18	Room temperature bottom part (additive)	ATHLET, CFX	−2.2	2.2	
19	HTC insulation outer wall to air (value)	ATHLET, CFX	2.1	8.2	
20	HTC ball valves (value)	ATHLET	2.1	8.2	
21	HTC EPM pump (value)	ATHLET	2.1	8.2	
22	Initial mass flow rate in TS leg (additive)	ATHLET	−0.0594	0.0592	S301.03
			−0.0187	0.0326	S301.04
			−0.03	0.0302	S310.01

Table 7
TUM – List of uncertain input parameters and their ranges.

#	Parameter	Code	pdf	min	max
1	Roughness of pipes in MH-leg (value)	ATHLET	UNIFORM	1.69E-05	2.63E-05
2	Roughness of pipes in common parts (value)	ATHLET	UNIFORM	1.69E-05	2.63E-05
3	Roughness of pipes in HX-leg (value)	ATHLET	UNIFORM	1.69E-05	2.63E-05
4	Roughness of pipes in 3D-leg (value)	ATHLET	UNIFORM	1.91E-05	2.85E-05
5	Roughness of pipes in Rotamass (value)	ATHLET	UNIFORM	1.69E-05	2.63E-05
6	Roughness of pipes in 3D test section	ATHLET	UNIFORM	1.91E-05	2.85E-05
7	Power of the main heater (factor)	ATHLET	UNIFORM	0.977	1.023
8	Power of the 3D heater (factor)	ATHLET, CFX_InDeck	UNIFORM	0.985	1.015
9	PFL coefficients in MH-leg (factor)	ATHLET	UNIFORM	8.13E-01	1.23E + 00
10	PFL coefficient EPM-pump (value)	ATHLET	UNIFORM	29.267	41.735
11	HTC in common parts (factor)	ATHLET	UNIFORM	0.9	1.1
12	HTC in HX-leg (factor)	ATHLET	UNIFORM	0.9	1.1
13	HTC in MH-leg (factor)	ATHLET	UNIFORM	0.9	1.1
14	HTC in 3D-leg (factor)	ATHLET	UNIFORM	0.9	1.1
15	HTC forced or natural convection to LBE	ATHLET	UNIFORM	0.85	1.15
16	HTC insulation outer wall to air	ATHLET, CFX_InDeck	UNIFORM	2.1	8.2
17	HTC ball valves	ATHLET	UNIFORM	2.1	8.2
18	HTC EPM-pump	ATHLET	UNIFORM	2.1	8.2
19	Initialization temperature at TC1.0000 (additive)	ATHLET	UNIFORM	−2.2	2.2
20	Room temperature bottom part (additive)	ATHLET, CFX_InDeck	UNIFORM	−2.2	2.2
21	LBE dynamic viscosity (multiplicative)	ATHLET, CFX_InDeck	UNIFORM	0.92	1.08
22	LBE thermal conductivity (multiplicative)	ATHLET, CFX_InDeck	UNIFORM	0.95	1.05

- Underestimation of the flow in the 3D leg. Considering close to stagnant flow in the 3D leg, small error can have important effect on flow temperatures.
- Application of a model that has not been calibrated against tests with a continuous negative flow in the 3D leg.
- Experimental uncertainty in the mass flow rate measurement.

Both participants have correctly predicted flow direction in MH and 3D legs in natural circulation. Transient mass flow rates are captured better by CEA; however, the final steady state in terms of both mass flow rates and flow temperatures are better predicted by ENEA. The flow temperature at the outlet of the test section (TC2.1211) is underestimated in the ENEA simulations, interestingly, it seems to have no effect on other loop sections suggesting that miss-calibration of the test section is compensated in other parts of the loop.

Simulations by GRS and TUM were performed using ATHLET. In presented simulations GRS generated the input models for ATHLET and ANSYS CFX. TUM performed uncertainty quantification based on provided models. The uncertainty ranges were established using 1st order Wilks method with 95/95% confidence level and tolerance interval. The model input parameters were assumed to be independent and a uniform distribution was used for sampling; respective input ranges are given in Table 6.

The input ranges for the parameters in Table 6 (as well as in

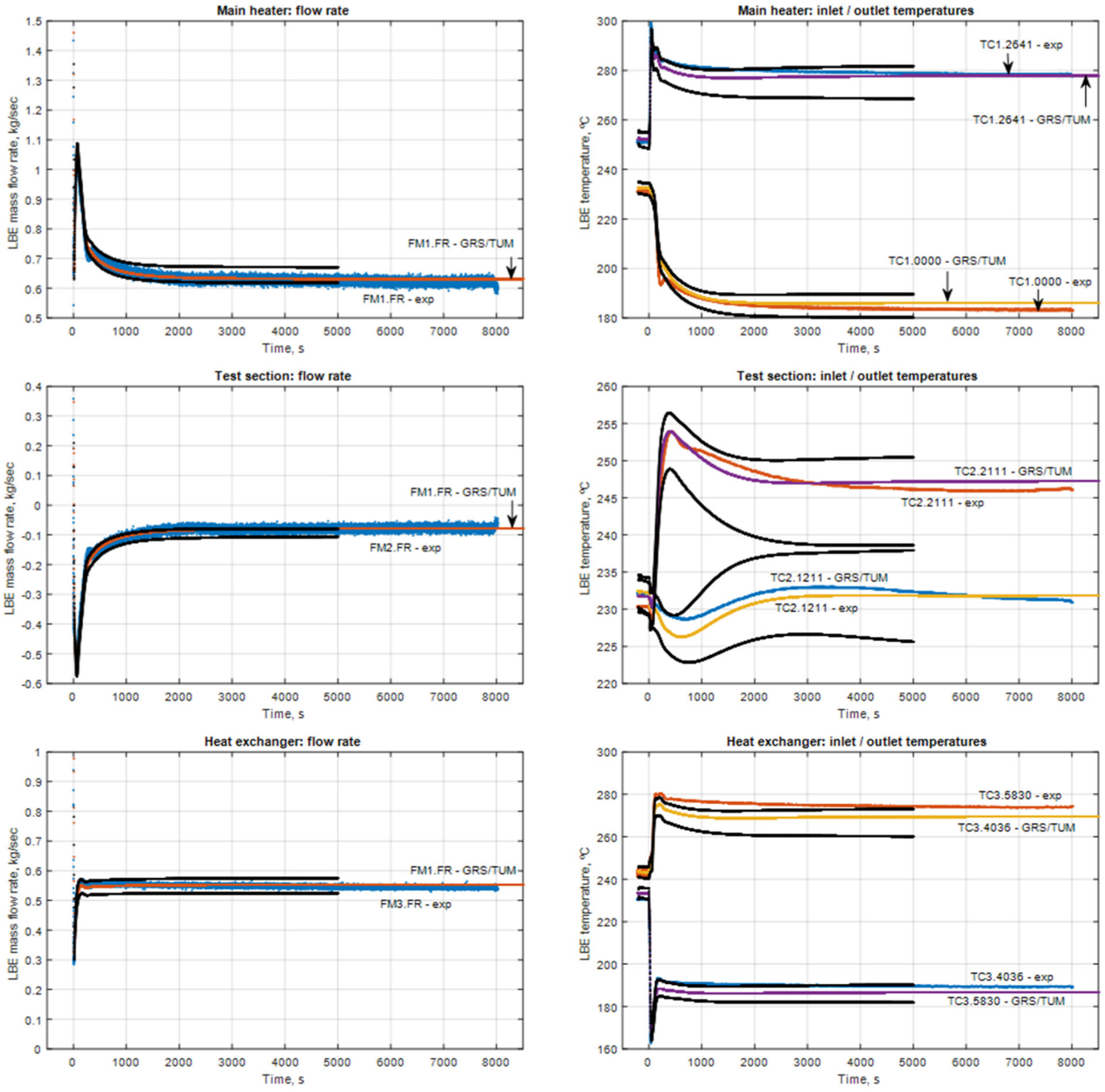

Fig. 7. GRS/TUM simulations of the open STH benchmark (TG03.S310.01). (black lines in the plots show lower and upper bounds from UQ).

Table 7) were selected in the following manner:

- wall roughness, heaters power, and initialization temperature were specified based on reported experimental uncertainty;
- LBE physical properties were specified according to the uncertainty bounds found in (Stieglitz, 2007);
- PFL coefficients were varied so that the mass flow rate in the 3D and HX legs would take values matching the experimental measurement with uncertainty;
- HTCs for insulation outer wall, ball valves and EPM pump were taken conservatively large;
- HTCs for matching heat flux from the MH and test section heater in forced and natural circulation were obtained using constrained optimization while varying the target value within experimental uncertainty;
- other HTC were taken with ± 10% uncertainty range from the best

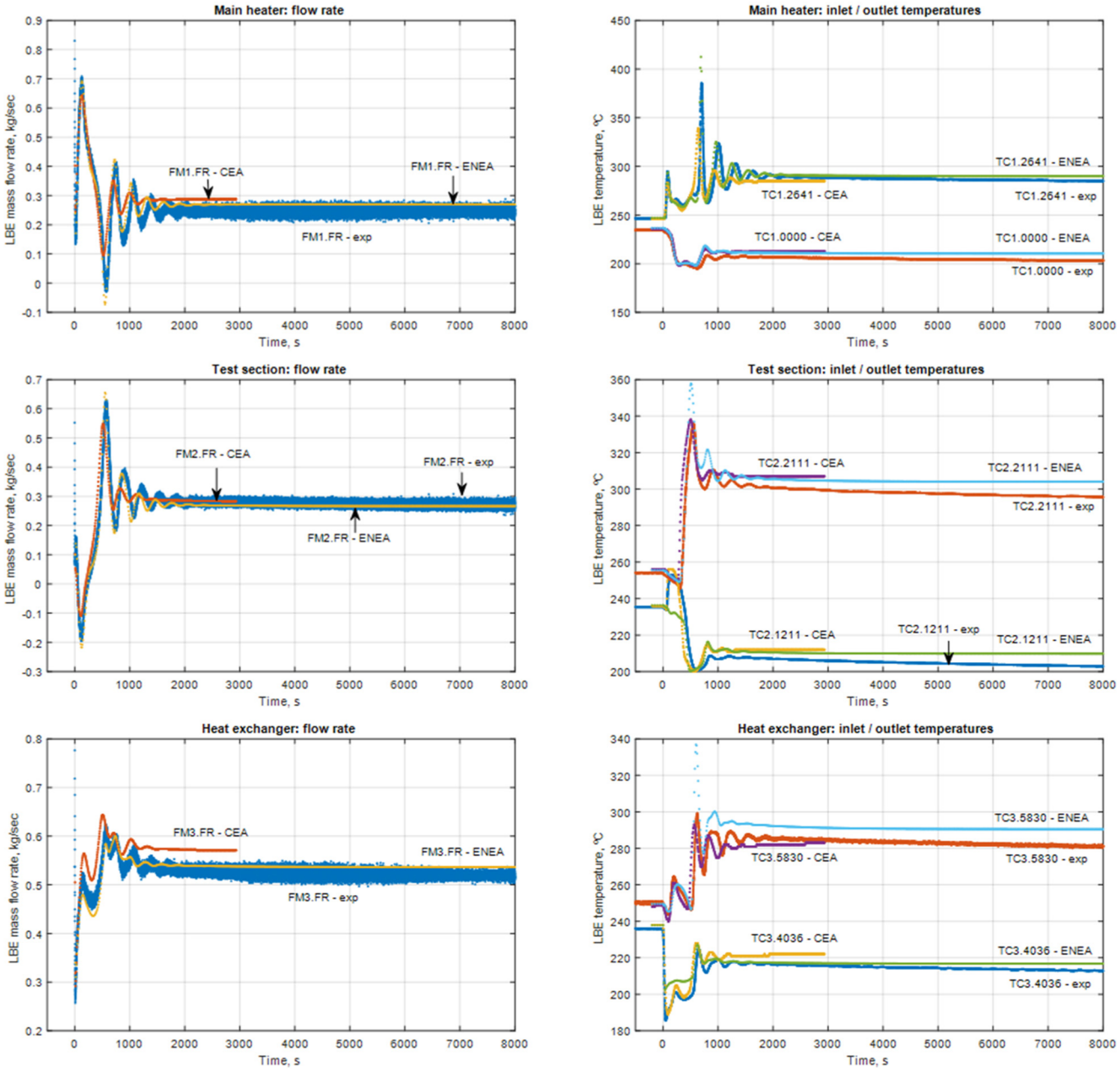

Fig. 8. CEA and ENEA simulations of the TG03.S301.04.

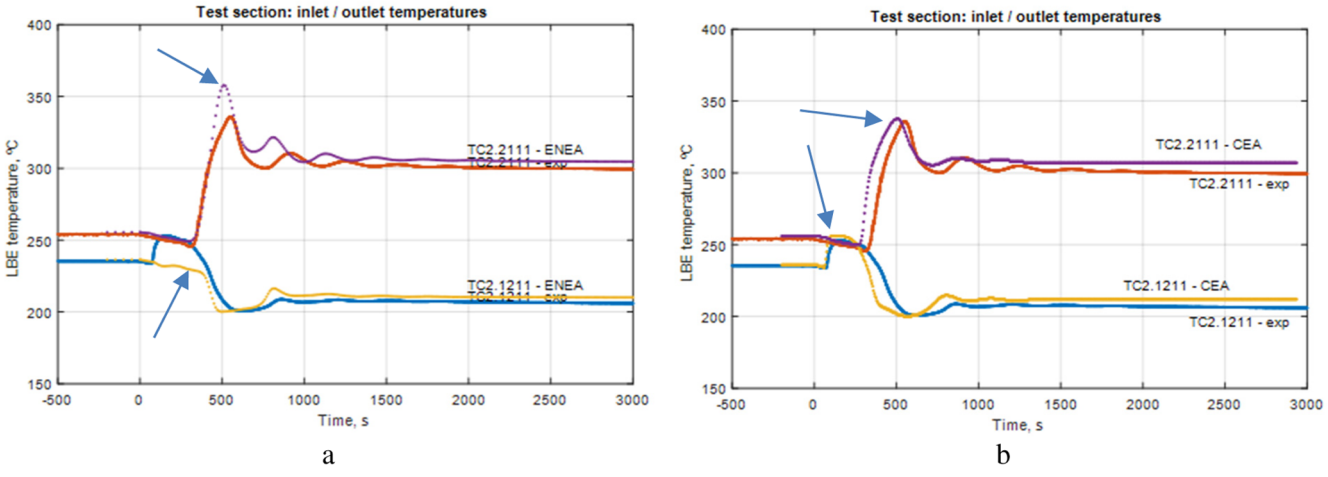

a b

Fig. 9. Results of open coupled STH/CFD benchmark test simulations TG03.S301.04. (a – ENEA; b – CEA).

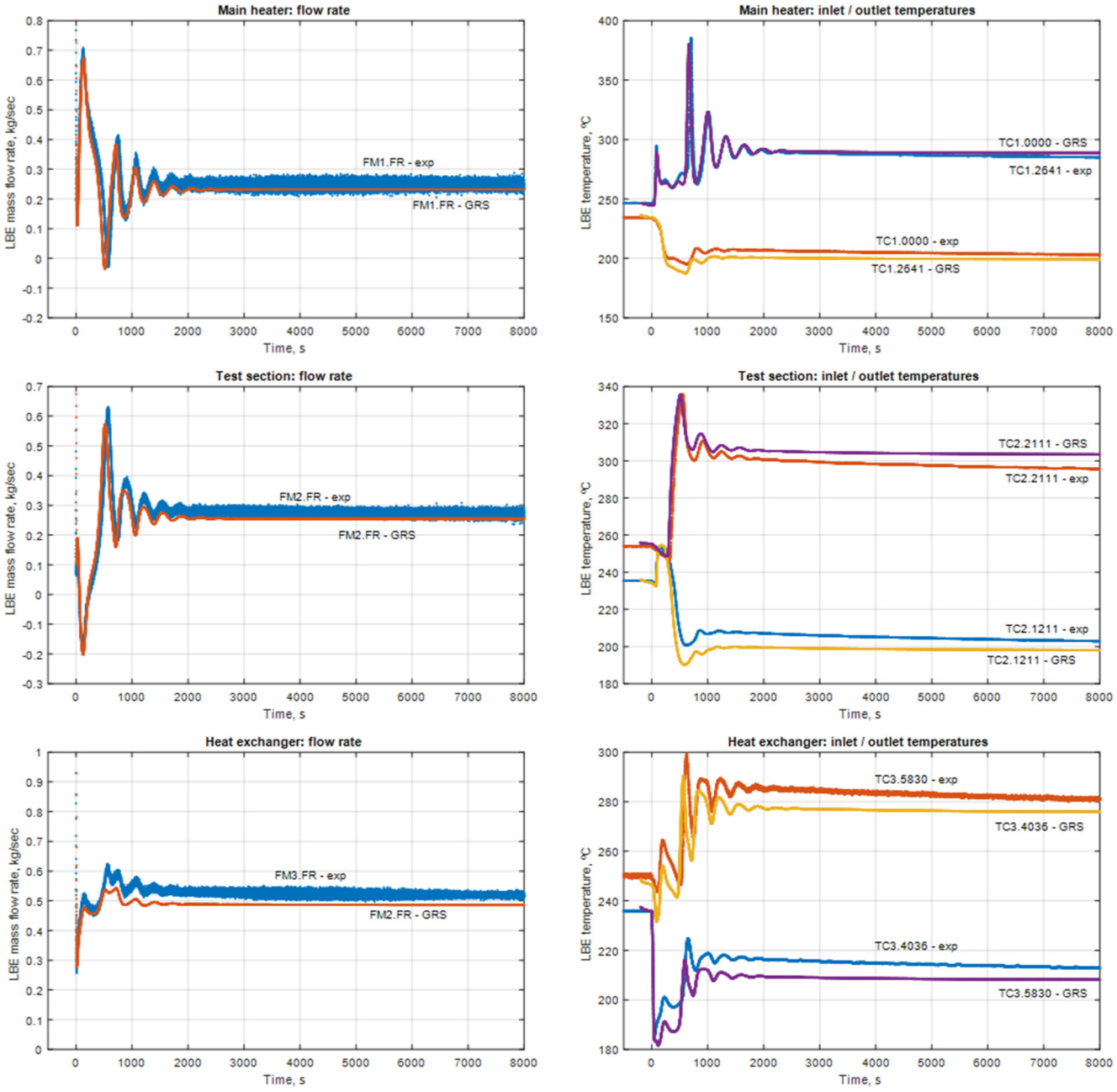

Fig. 10. GRS simulations of the coupled STH/CFD benchmark TG03.S301.04.

estimate value.

The results of the best estimate simulation and uncertainty quantification are provided in Fig. 7. ATHLET predicted very well the LBE mass and temperature distribution in the facility over the entire experiment. The maximum temperature deviations are within 5–6 K, while the mass flow rates lie within the measurement uncertainty of 0.03 kg/s. Furthermore, the transient dynamics is also well represented by ATHLET. Some deviation is found in the transient progression of the TS outlet temperature. The detailed analysis of this transient with ATHLET can be found in (Papukchiev et al., 2019). The uncertainty bounds encompass experimental data demonstrating model validity for the considered type of transient (S310). The results suggest high sensitivity of flow temperature in the test section leg to the model input uncertainty. This effect is due to the low mass flow rates in the 3D leg, specific to this test.

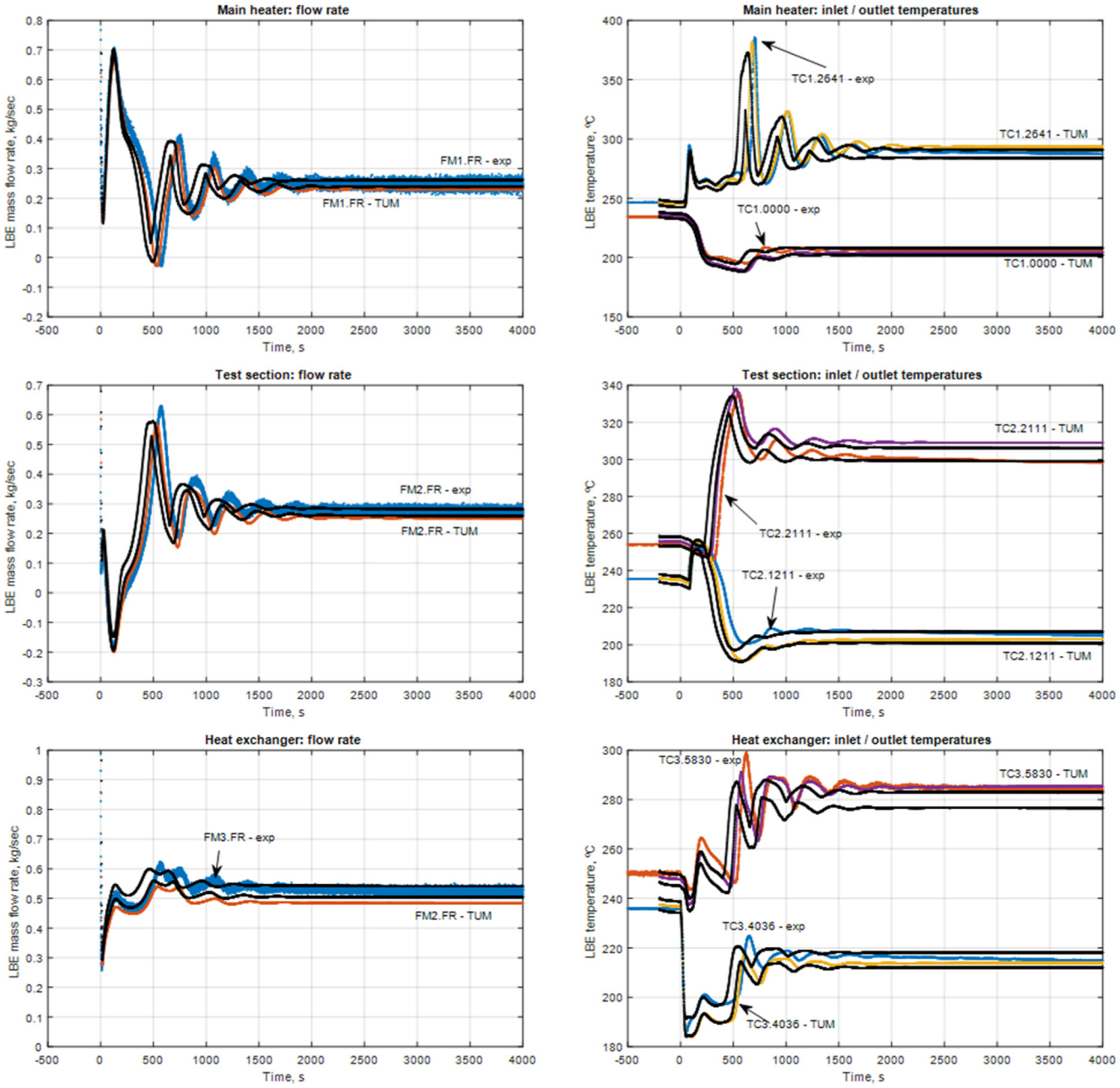

Fig. 11. TUM simulations of the open coupled STH/CFD benchmark TG03.S301.04. (black lines in the plots show lower and upper bounds from UQ).

4.2. TG03.S301.04 – STH or coupled STH/CFD code benchmark

ENEA has selected standalone CATHARE and CEA used coupled CATHARE/TRUST to model TG03.S301.04 transient. Modelling uncertainty has not been quantified. Both simulations compare well with experimental data (see Fig. 8). However, the ENEA model fails to reproduce the temperature rise at the inlet to (TC2.1211) the test section during the flow reversal (Fig. 9a) and consequently overestimates the peak temperature at the test section outlet (TC2.2111) during flow recovery. Coupled simulations are necessary to correctly capture temperature profile in the test section pool and consequently temperature at the test section inlet and later outlet (Fig. 9b). Both models find the steady state solution at slightly higher average flow temperatures than in the experiment. However, the deviation is relatively small – around 10 K in all three legs. The steady state temperatures seem to be better predicted in ENEA calculations.

For the simulation of the TG03.S301.04 transient GRS developed a coupled ATHLET/ANSYS CFX model and TUM has performed

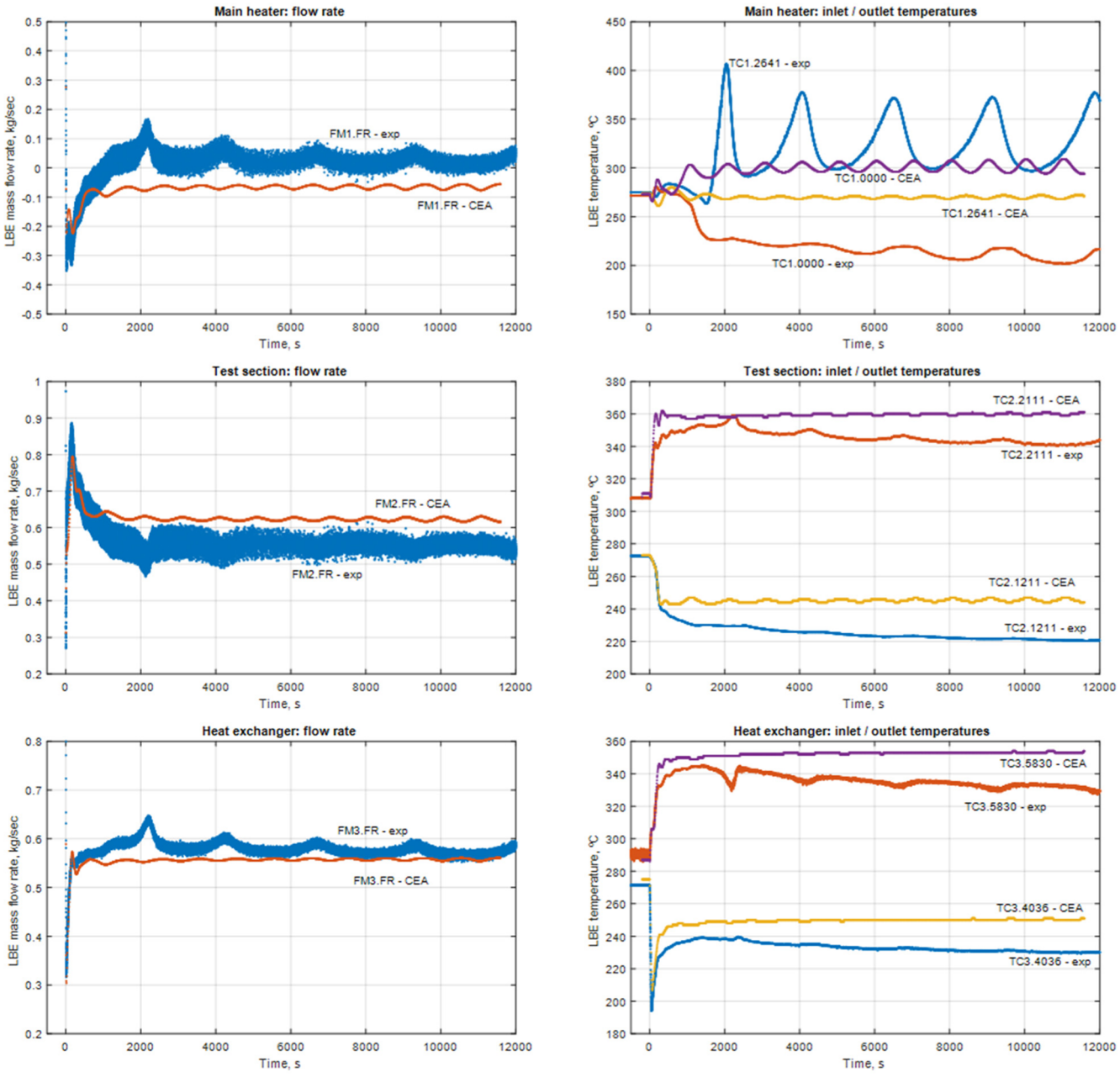

Fig. 12. CEA – Coupled simulations of the blind benchmark TG03.S301.03 (blind phase).

uncertainty quantification. The list of input uncertain parameters and their ranges can be found in Table 6. Wilks 1st order method with 120 runs was used to provide two sided 95% tolerance interval with 95% confidence level. The uncertainty bounds represent min/max of the 120 simulations and therefore do not belong to a single simulation.

The results of GRS simulation of TG03.S301.04 (see Fig. 10) are slightly different from TUM best estimate (Fig. 11) in spite the fact that both partners used similar coupled model. Both simulations though reproduce well the experiment. Results in Fig. 11 suggest that experimental simulation falls inside the uncertainty bounds through the entire transient with the exception of few temperature peaks and flow temperature at the inlet to HX (TC3.5830). The results allow to consider the model by GRS/TUM as capable to predict S301 type of transients.

4.3. TG03.S301.03 – semi-blind benchmark test (blind phase)

The CEA simulation (Fig. 12) predicts reversed flow (− 0.065 kg/s) in the MH leg – opposite to the one in the experiment (+ 0.035 kg/s). While the absolute difference is hardly exceeding 0.1 kg/s – qualitatively the test was not captured. In spite of that, the simulation does predict natural circulation instability (similar to LCO) in the MH leg but for downwards flow and indicates that a different type of transient behaviour might be possible in TALL-3D facility.

The ENEA standalone STH modelling (Fig. 13) has predicted a

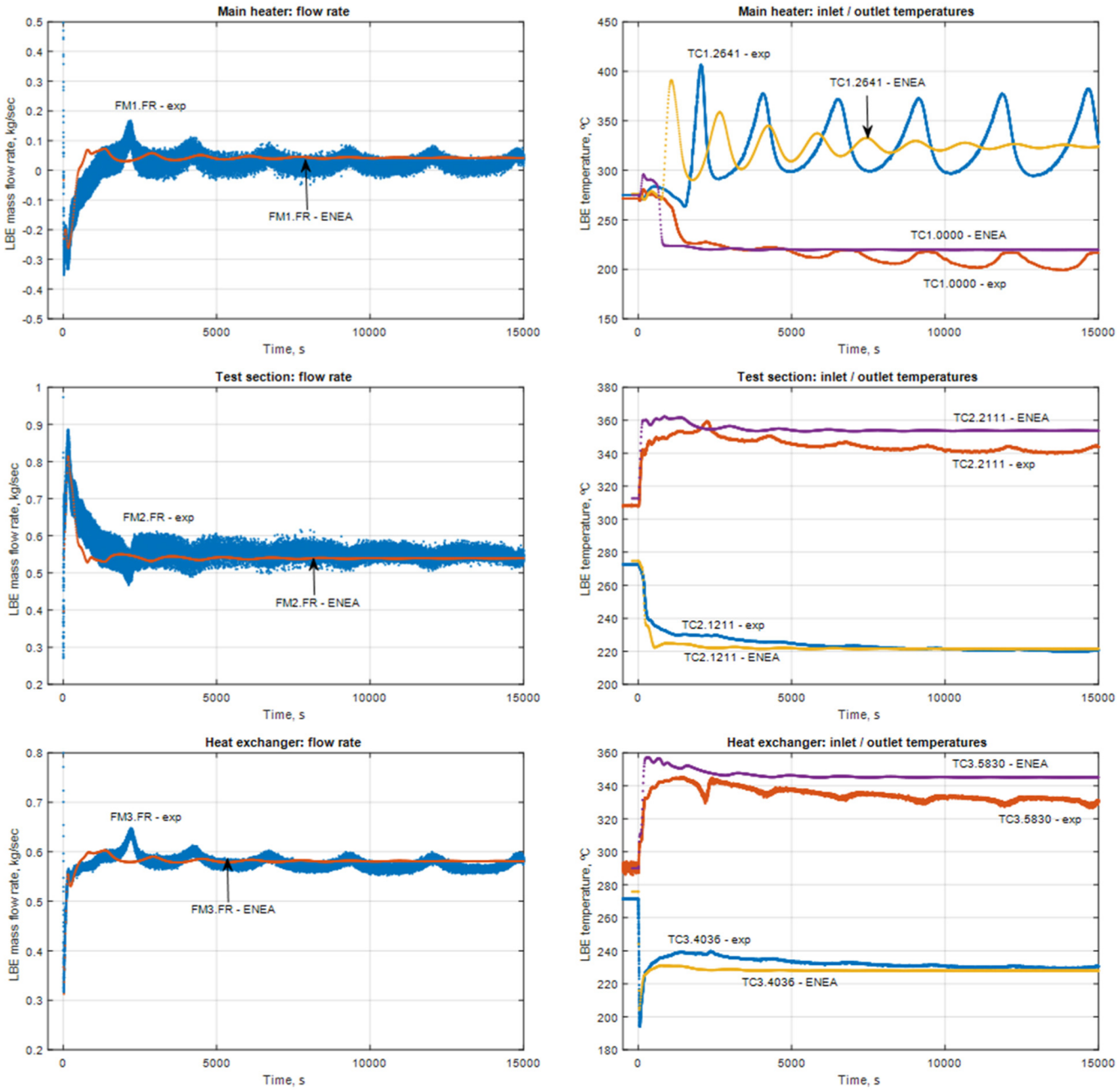

Fig. 13. ENEA – STH simulations of the blind benchmark TG03.S301.03 (blind phase).

standard forced to natural transient with reducing flow and temperature oscillations, which is qualitatively different from the experiment. The estimated magnitudes of the mass-flow rates compare well with the experiment. In general, the developed by ENEA and CEA models seem to be well calibrated, however, without uncertainty analysis it is difficult to judge whether these models can capture the actual transient phenomena of the TG03.S301.03 test.

The GRS results (coupled simulations) are provided in the Fig. 14. The predicted magnitudes of the mass flow rates in all three legs agree well with the experiment, except for the mass flow rate peaks. In addition, the estimated amplitude of the temperature oscillations in the MH leg is increasing similar to the experiment. However, the frequency of temperature and flow oscillation are underestimated causing longer flow stagnation in the MH and much higher magnitude of temperature oscillations in the MH outlet, which then propagates throughout other model sections. The average temperature in the simulations is higher than in the experiment. According to GRS, the main reason for the discrepancies is due to the modelling uncertainties related to the form

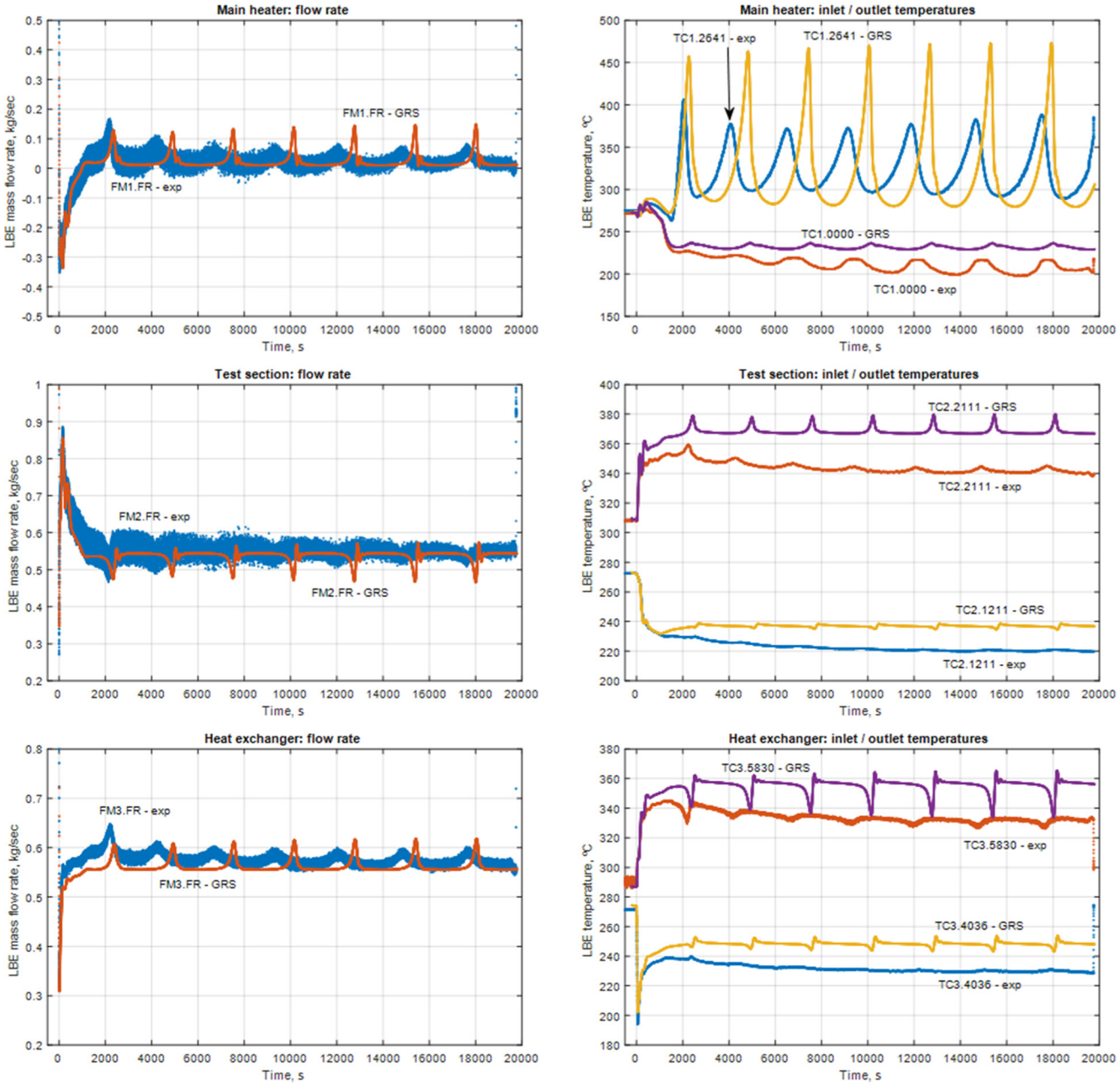

Fig. 14. GRS – Coupled simulations of the blind benchmark TG03.S301.03 (blind phase).

loss coefficient in the electromagnetic pump, the transferred power through the HX (water instead of oil in the secondary side), and the heat losses. A detailed analysis of the semi-blind and open phases can be found in (Papukchiev et al., 2019).

The simulation of the blind benchmark was also performed by TUM. TUM has used the model from GRS and has obtained the same best estimate results. TUM supplemented their simulation with uncertainty propagation. Using random sampling, 59 simulations have been performed on the coupled model input. Applying 1st order Wilks formula two sided tolerance limits were reported. The sampling was performed in the space of 22 input parameters, their list and ranges can be found in the Table 7. Those parameters include thermal losses (11–18) and surface roughness (1–6) in different sections, electric power of the MH and test section (7–8), temperature offsets (19–20), pressure flow loss coefficients (9–10) and some others. Notice that ranges of uncertainty vary for different parameters from ± 2.5% to ± 50%.

The results of the uncertainty propagation for the mass flow rates and primary loop temperatures are provided in the Fig. 15. The data

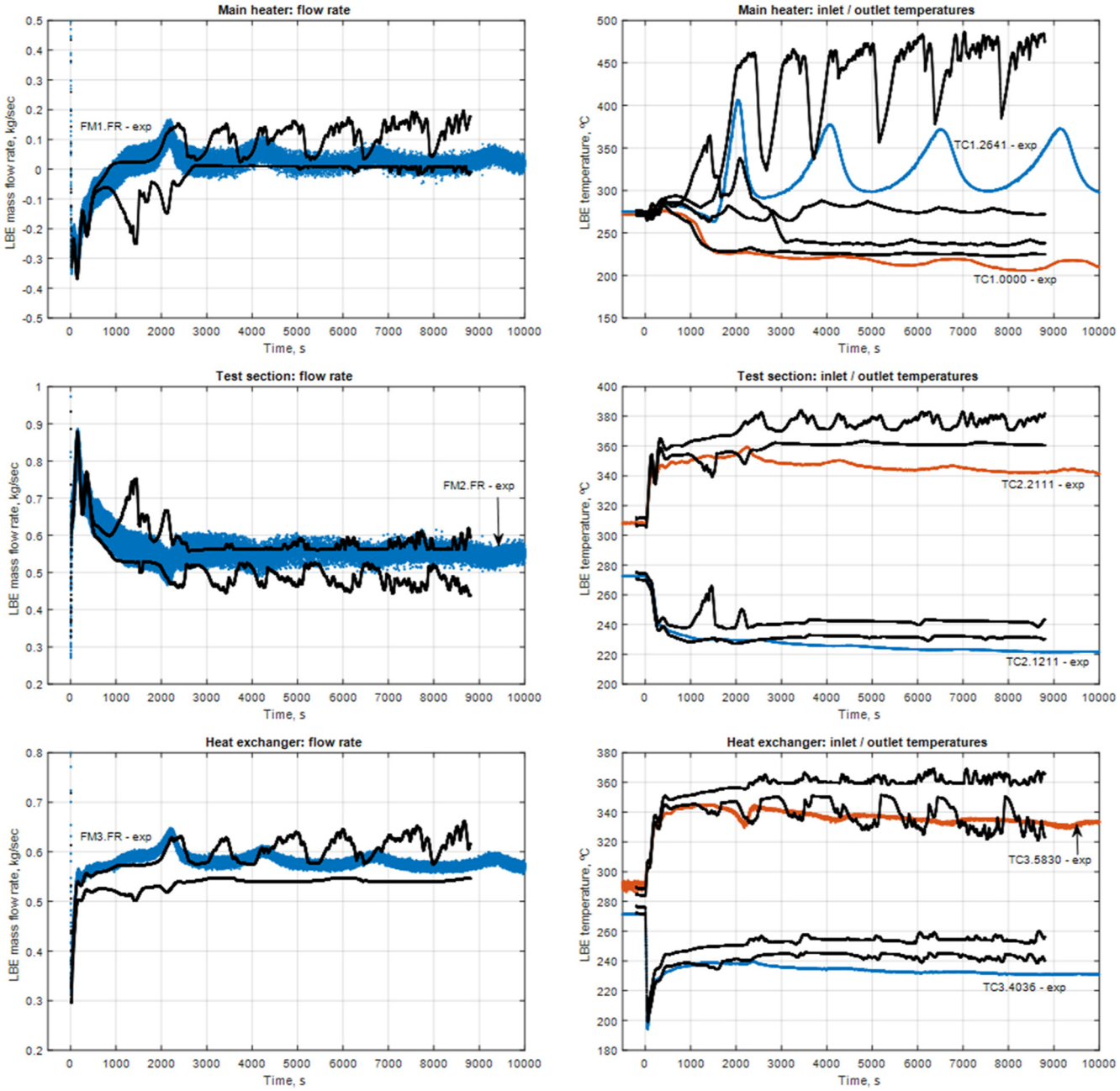

Fig. 15. TUM – Coupled simulations of the blind benchmark – 91/95 two-sided tolerance limits (blind phase).

suggest that effect of the input uncertainty is dominant for the loop temperatures and is less important for the LBE mass-flow rates. Reduction of the noise in the measurement of the mass flow rates could be recommended to help reduce modelling uncertainty. The predicted uncertainty ranges for flow temperature in most cases do not encompass experimental data (even taking into account experimental uncertainty) suggesting that either the list of uncertain input parameters is incomplete or parameters ranges are taken too narrow. The chaotic character of the time evolution of the upper and lower limits implies that for given input uncertainty the model may predict different types of transients.

The results of the pool modelling are demonstrated in Fig. 16. The data suggests that in simulation (i) temperatures in the pool are somewhat overestimated and (ii) thermal stratification is more pronounced. This could be attributed to the underestimation of thermal losses in the 3D domain.

4.4. TG03.S301.03 – semi-blind benchmark test (open phase)

The results from ENEA in the open phase of the semi-blind

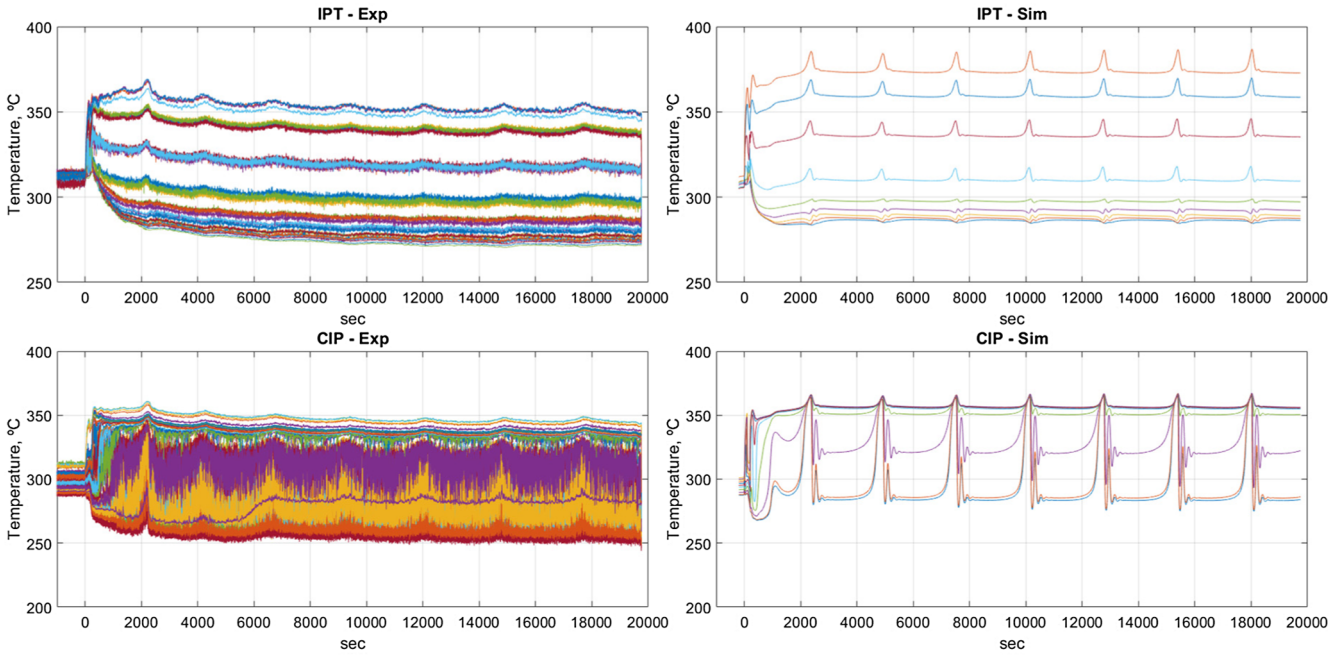

Fig. 16. GRS/TUM – Coupled simulations of the blind benchmark – TALL-3D pool temperatures (blind phase).

benchmark (see Fig. 17) are only marginally different from the results demonstrated in the blind simulation. The possible reason is difficulty to recalibrate input model when there is no natural circulation steady state commonly used for model "fine tuning" to a specific transient.

In the open phase of the blind benchmark GRS and TUM used different coupled (ATHLET/ANSYS CFX) input models for the simulations. The best estimate results are compared to the experiment in Fig. 18. The mass flow rates and flow temperatures are captured well by both models in 3D and HX legs. The main focus is therefore on the MH leg. Here the GRS model shows noticeable improvement compared to the blind phase and fits better the experimental data than the model by TUM. Specifically, TUM model predicts dampening flow temperature oscillations characteristic for majority of S301 transients. GRS model on the other hand shows limit cycle oscillations reproducing experimental data; however, the growing amplitude of the temperature oscillations that can be seen in the experiment after ~10000 s is missed. Both simulations do not capture well the frequency of the temperature and mass flow oscillations.

TUM has additionally performed uncertainty analysis for the coupled model (see Fig. 19). The uncertainty bounds do not always encompass experimental data and it is not obvious if individual simulations reproduce the characteristic transient behaviour.

TUM has further attempted to run standalone STH simulations of the transient using ATHLET code. As it can be expected and was already explained the results do not differ much from the coupled simulations (see Fig. 20).

5. Lessons learned

The ultimate goal of validation benchmarking is to demonstrate code predictive capability for the intended use and identify possible user effects. In order to evaluate the benchmark results, it is important to

- report model calibration in a transparent manner, i.e. to justify selection of the ranges of uncertain input parameters, make sure these ranges were presumed between benchmark tests and be able to identify the key factors dominating model output uncertainty
- design the benchmark and respective open/blind phases of the benchmark to limit potential for "overfitting" of the model input, i.e. data used for input calibration should be obtained in significantly different conditions than the validation data.

The results of this benchmark exercise suggest that, when thoroughly calibrated, input models can satisfactory reproduce experimental data from TALL-3D and uncertainty quantification encompasses experimental data. However, in case of insufficient input calibration best estimate simulations may miss-predict test results qualitatively. In any case predictive capability of the model can be judged only using detailed uncertainty analysis.

The following lessons can be outlined from this work:

- Uncertainty analysis is a very important part of benchmark simulations:
  - o Both open and blind benchmarks best estimate results are subject to "user effect". Without uncertainty analysis open benchmark phase becomes a "fitting" exercise, given complexity of the problem and a number of adjustable parameters, more efforts in fitting is likely to provide better results. Such fitting, however, doesn't really address code predictive capabilities and the influence of uncertainties.
  - o Benchmarking must be preceded with well described and demonstrated model calibration stage. The goal of such demonstration is to identify main sources of the modelling uncertainty and provide evidence for selection of the uncertainty ranges for the most influential model input parameters.
  - o It is important to focus on ranges for uncertain input parameters, rather than variation of the parameters around best estimate

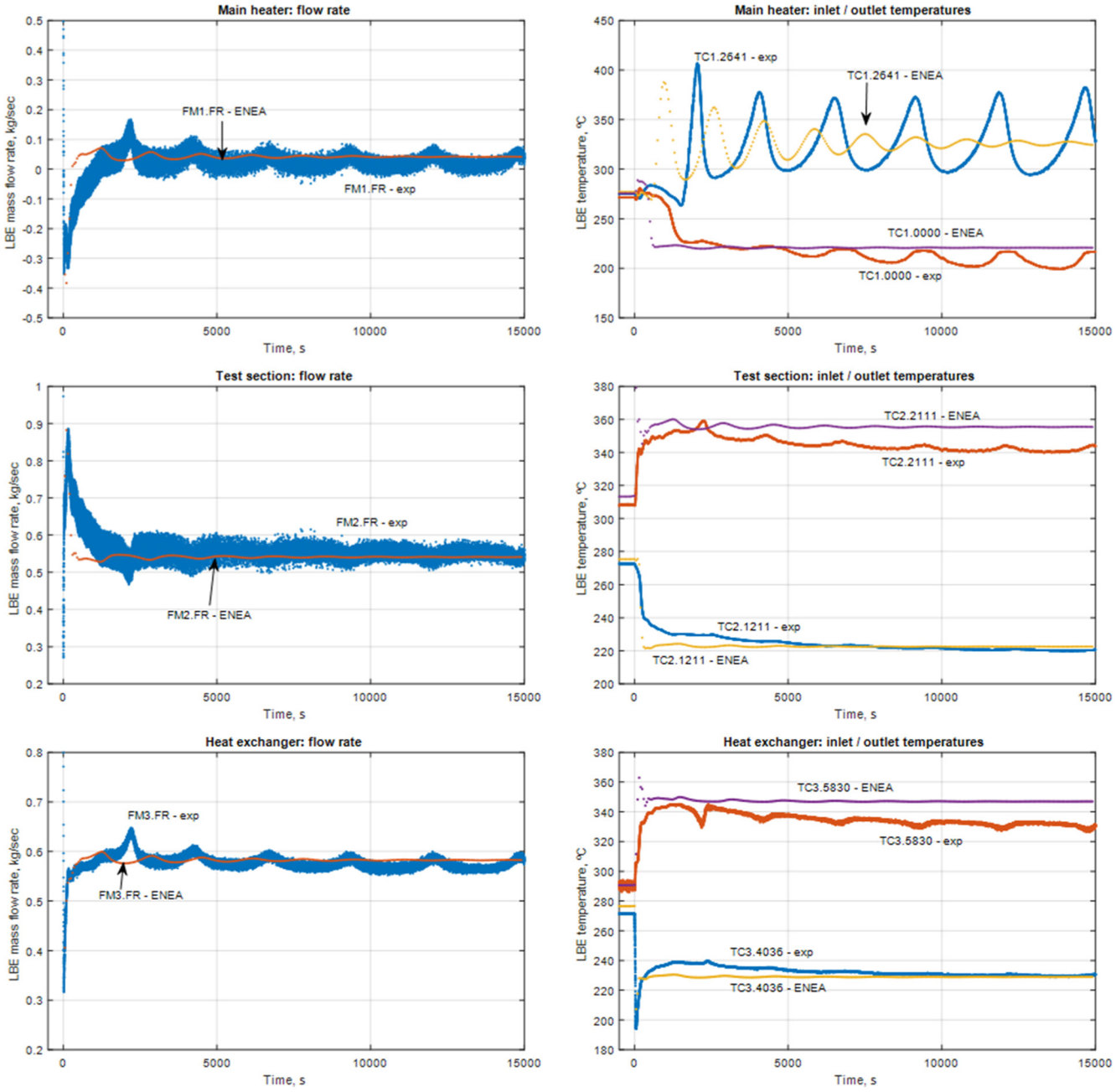

Fig. 17. ENEA – STH simulations of the blind benchmark TG03.S301.03 (open phase).

values, e.g. 123 ± 5%. In such case, modification of the best estimate value (1 2 3) will alter the uncertainty range of the respective parameter.

- Selection of calibration tests:
  - o Calibration tests must cover all relevant phenomena and regimes of the experimental setup, especially if such phenomena will be presented in the benchmark tests.
  - o Calibration tests shall include (besides integral tests) separate phenomena tests to minimize the possibility of self-compensating errors in calibration of different parts of the model.
  - o Number of calibration tests must be sufficient to assess independently ranges of each uncertain input parameter.
  - o Approach and results of calibration must be reported for each input model used in the benchmarking or validation.
- Selection of benchmark tests:
  - o Benchmark tests can feature new phenomena that have not been considered in the model calibration, only if those phenomena do not introduce the need for calibration of additional input parameters.
  - o For each important phenomenon, every open benchmark should be generally complemented with a blind benchmark to understand the degree to which model input calibration can mask

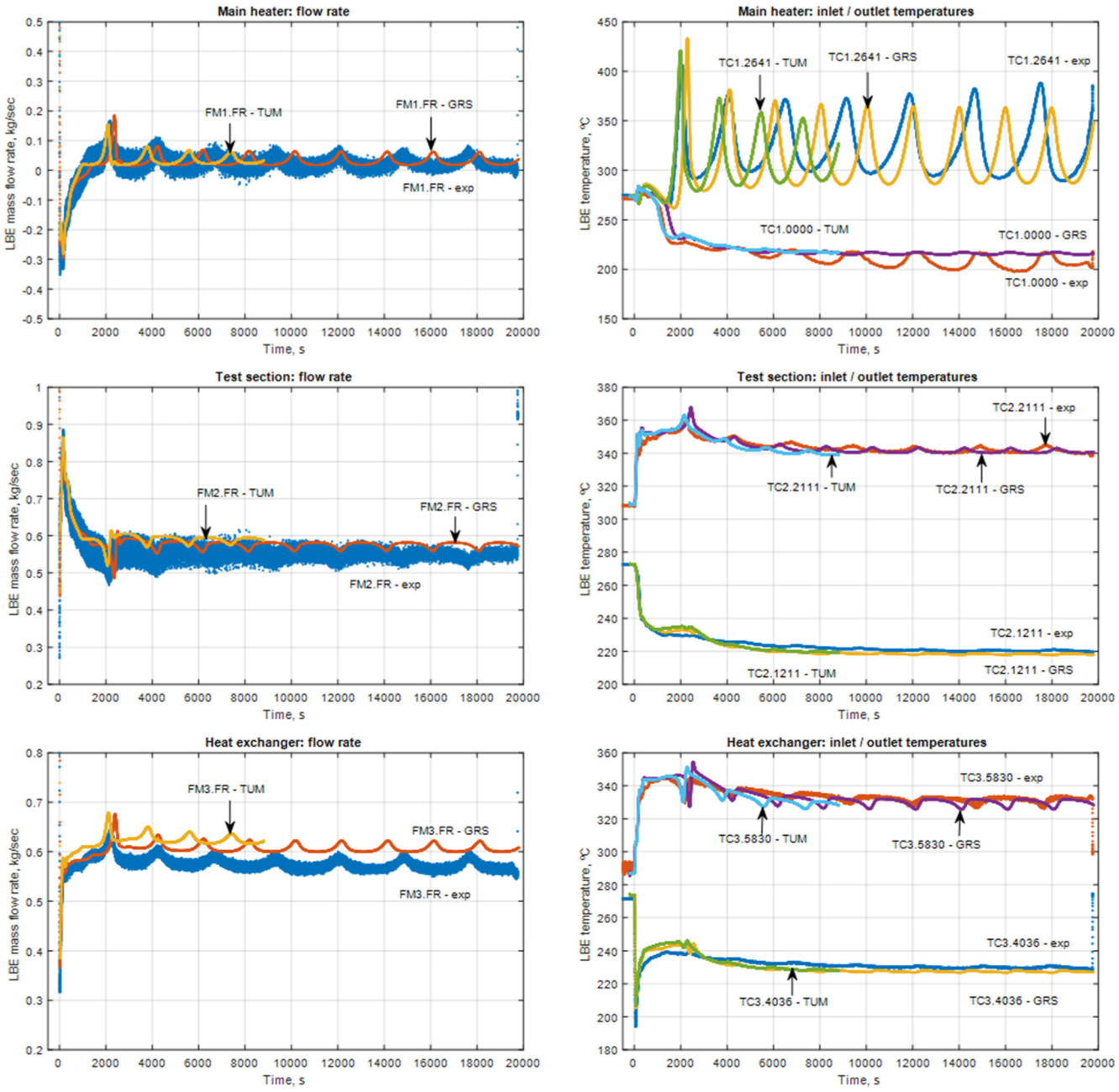

Fig. 18. GRS and TUM results – Coupled simulations of the blind benchmark (ANSYS CFX + ATHLET) (open phase).

potential deficiencies of the models.

- o Benchmark transients with several changes in boundary conditions can be an effective approach to understanding of the model predictive capability and possible "overfitting" in the calibration process.
- o To be more informative open benchmark shall separately test individual (STH and CFD) and coupled (STH/CFD) models. This step can be taken further and applied to individual sections of the experimental facility (e.g. benchmarks for Heat Exchanger, Main Heater and Test section pool). Such approach while more demanding may provide a more adequate picture about individual models and codes maturity.

- Definition of validation metrics, i.e. required level of agreement between the experimental and modelling SRQs:
  - o Questions of model intended use and scaling issues should be explicitly considered in the benchmarking process.
  - o Definition of the validation metrics must be multidimensional to account for the necessity of simultaneous capture of multiple SRQs and shall include both steady state and transient characteristics.

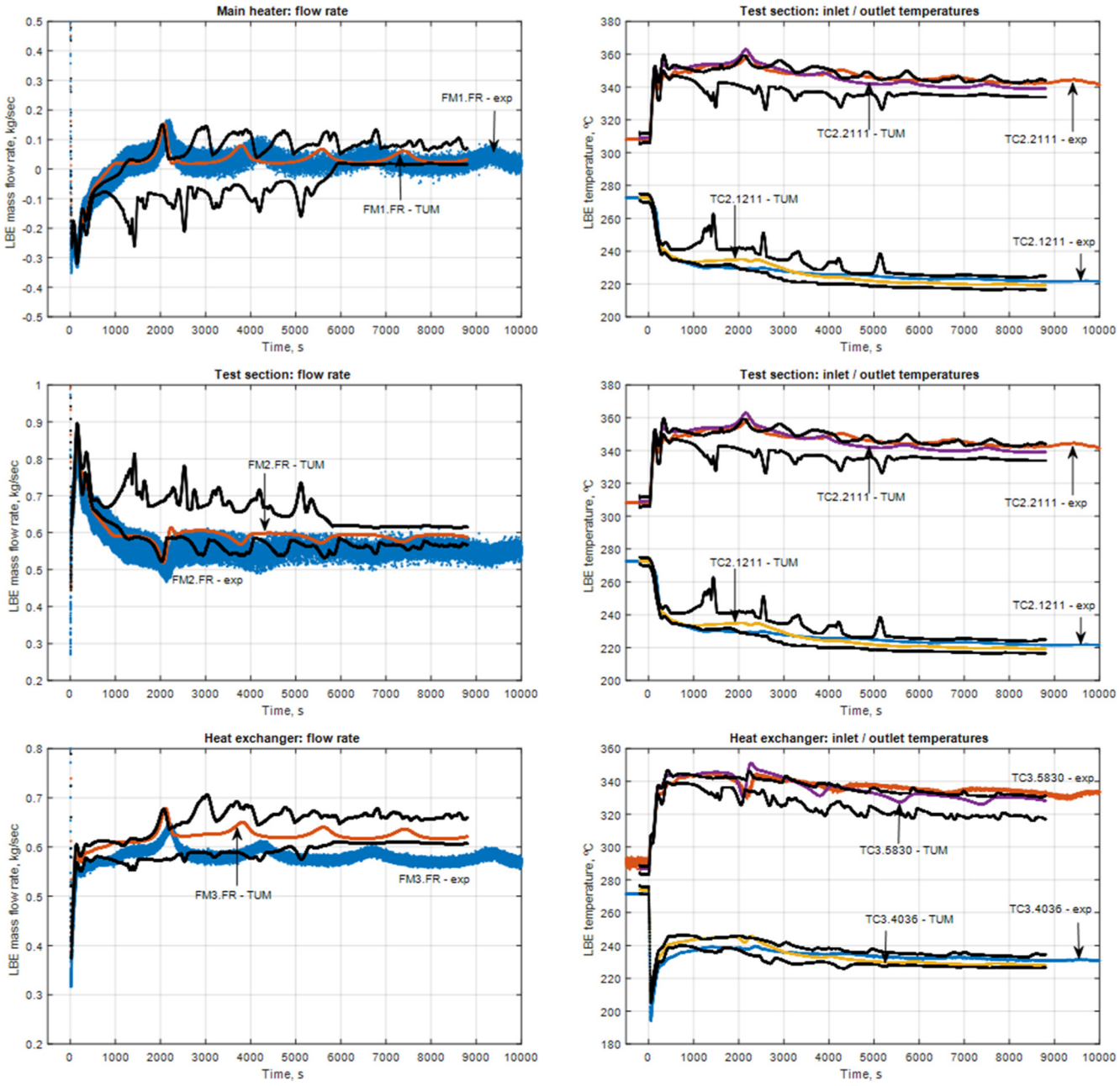

Fig. 19. TUM uncertainty analysis – blind benchmark (ANSYS CFX + ATHLET) – 95/95% tolerance limits (120 runs) (open phase).

- o In a closed system with feedbacks, wrong calibration of some parts of the model input can be effectively compensated by wrong calibration of other parts of the model input providing "on average" good integral results. In order to identify such deficiency, the benchmark metrics must have cumulative nature that incorporates separate metrics for different sections of the experimental setup.

- A systematic approach for model validation and reporting of the results to be followed for:
  - o Model sensitivity analysis to justify the selection of the most important input parameters.
  - o Model calibration to justify the selection of ranges for uncertain input model parameters.
  - o Benchmark simulations including best estimate case (and all qualitatively different cases) and output uncertainty ranges.

6. Conclusions

The first series of TALL-3D benchmark has been successfully performed. The results of the open benchmark were encouraging and demonstrated the overall maturity of standalone and coupled codes especially considering the results with uncertainty quantification.

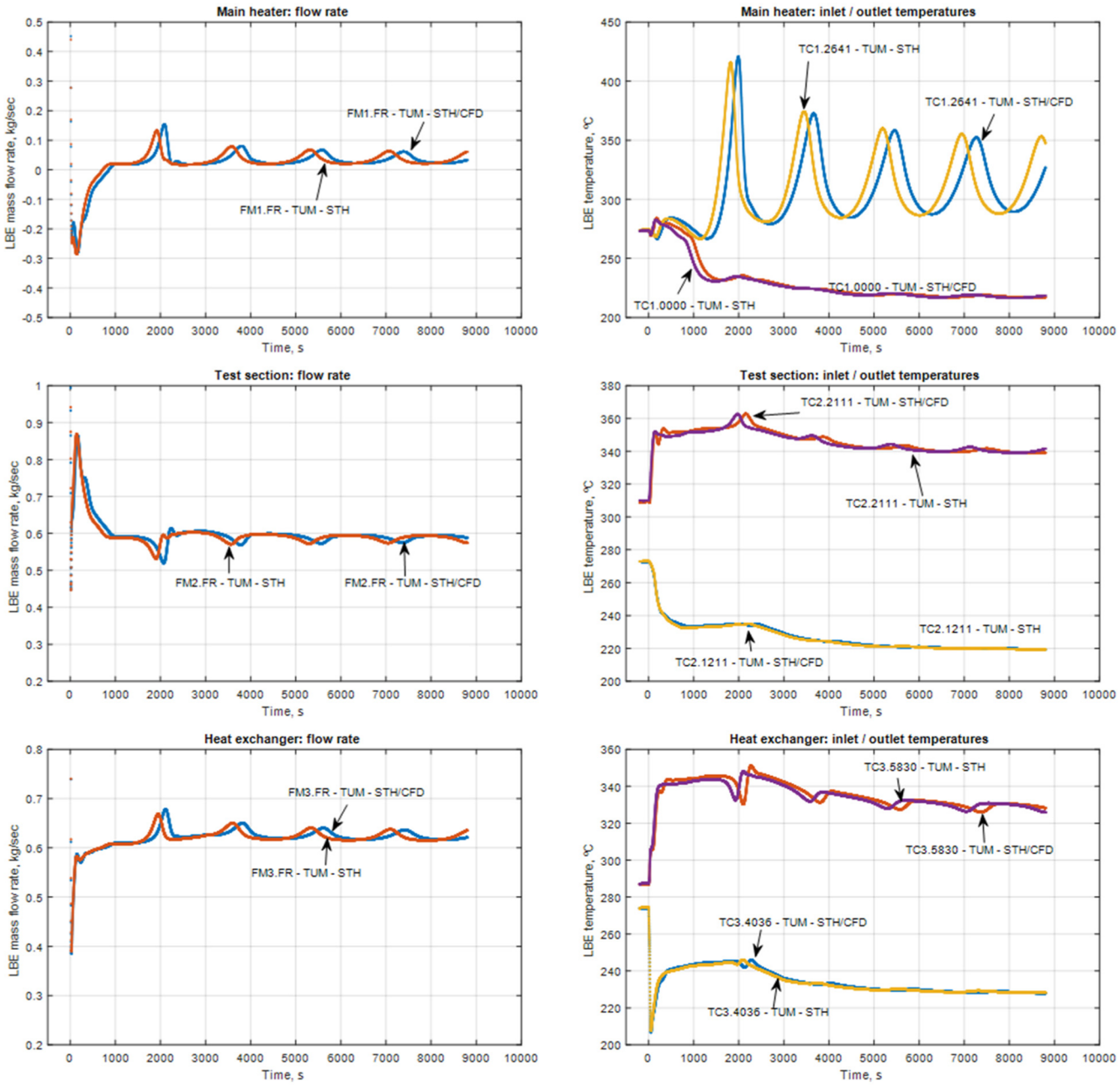

Fig. 20. TUM – blind benchmark TG03.S301.04 ATHLET vs ATHLET/ANSYS CFX (open phase).

Without uncertainty quantification it is difficult to judge about possible discrepancies between the experiment and simulation.

All participants were able to successfully predict TG03.S301.04 and GRS/TUM validated their model with uncertainty propagation. The transient TG03.S310.01 for "standalone" codes was correctly reproduced only by the GRS/TUM model suggesting that further model calibration might be needed for other partners.

The semi-blind benchmark has demonstrated a spread of the results. In fact, all possible types of transients, including a potentially new one (predicted by CEA), have been obtained in simulations. The results of uncertainty quantification presented by TUM/GRS suggest that the predictions are close to experimental data and do capture the character of the blind benchmark transient (natural circulation instability), however an additional calibration might be needed to obtain better quantitative agreement.

Acknowledgment

This work was supported by the Horizon 2020C Project SESAME (Thermal-Hydraulics Simulations and Experiments for the Safety Assessment of MEtal Cooled Reactors, grant agreement No. 654935).

References

Cadinu, F., Kudinov, P., 2009. Development of a "Coupling-by-Closure" approach between CFD and System Thermal-Hydraulics Codes. Proc. The 13th International Topical Meeting on Nuclear Reactor Thermal Hydraulics (NURETH-13). Kanazawa City, Ishikawa Prefecture, Japan, Paper N13P1238.

Gen-IV International Forum, Basis for the Safety Approach for Design & Assessment of Generation IV Nuclear Systems – Revision 1, GIF/RSWG/2007/002, 2008, p. 91.

Grishchenko, D., Jeltsov, M., Kööp, K., Karbojian, A., Villanueva, W., Kudinov, P., 2014. Design and commissioning tests of the TALL-3D experimental facility for validation of coupled STH and CFD codes. Nucl. Eng. Des. 290, 144–153.

Grishchenko, D., Kööp, K., Jeltsov, M., Mickus, I., Kudinov, P., 2017. TALL-3D

experimental test data for the first test series. SESAME Rep. D4, 6.
Jeltsov, M., Kööp, K., Kudinov, P., Villanueva, W., 2013. Development of a domain overlapping coupling methodology for STH/CFD analysis of heavy liquid metal thermal-hydraulics. 15th International Topical Meeting on Nuclear Reactor Thermal Hydraulics, NURETH 15. May 12–17, 2013, Pisa, Italy, Paper 466.
Kööp, K., et al., 2017. Pre-test analysis for identification of natural circulation instabilities in TALL-3D facility. Nucl. Eng. Des. 314, 110–120.
Papukchiev, A., Geffray, C., Grishchenko, D., Kudinov, P., 2019. Validation of the system thermal-hydraulics code ATHLET for the simulation of transient lead-bismuth eutectic flows. In: Proc. of the NURETH-18 conference, Portland, USA.
Papukchiev, A., Lerchl, G., 2009. Extension of the simulation capabilities of the 1D system code ATHLET by coupling with the 3D software package ANSYS CFX. Proc. of the NURETH-13 Conference, Kanazawa, Japan.
Papukchiev, A., Geffray, C., Grishchenko, D., Kudinov, P., 2019. Thermal-hydraulic investigations on the transition from forced to natural convection in a closed experimental loop. Proc. of the ICAPP 2019 Conference, Juan-les-Pins, France.
Robert, M., Farvacque, M., Parent, M., Faydide, B., 2003. CATHARE 2 V25: a fully validated CATHARE version for various applications. In: Proceedings of the tenth international topical meeting on nuclear reactor thermal hydraulics, (pp. 1CD-ROM). Korea, Republic of: KNS.
Schoeffel, P., Hristov, H., Lerchl, G., 2014. Towards multidimensional thermal-hydraulic simulations with the system code ATHLET. Proc. of 45th Annual Meeting on Nuclear Technology, Frankfurt, Germany.
Stieglitz, R., 2007. Instrumentation. Handbook on LBE alloy and Lead properties, Materials Compatibility, Thermal hydraulics and Technology. OECD/NEA.